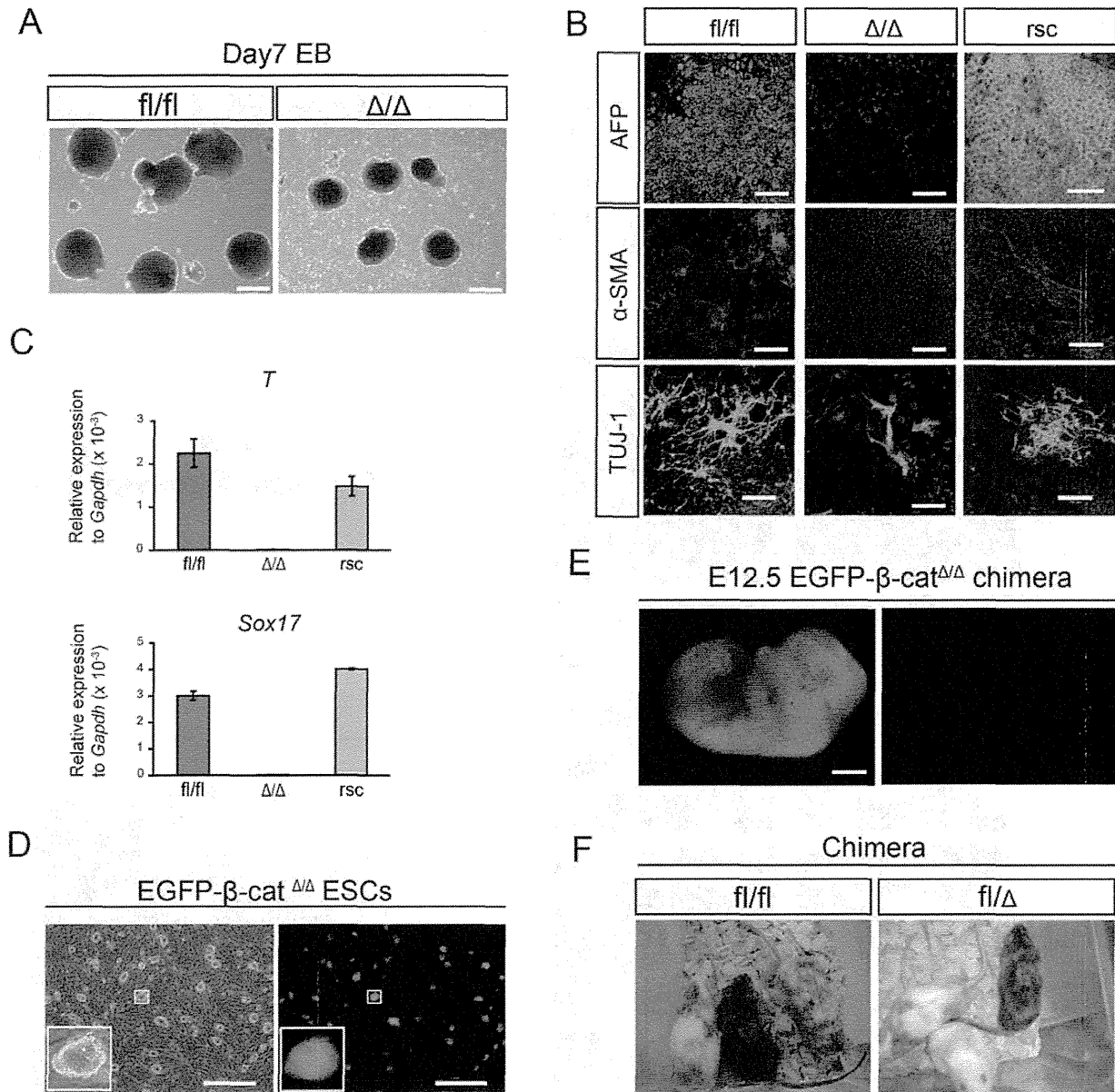


**Figure 1. Characterization of embryo-derived β-cat<sup>Δ/Δ</sup> mESCs.** (A): Morphological appearance of β-cat<sup>Δ/Δ</sup> mESCs is shown in the left panel. ALP staining of β-cat<sup>Δ/Δ</sup> mESCs is shown in the right panel. Scale bars are 150 μm. (B): Electrophoretic analysis of the genotyping PCR for wild-type (NCH4.3), β-cat<sup>f1/f1</sup> (f1/f11 and f1/f12), β-cat<sup>f1/Δ</sup> (f1/Δ2 and f1/Δ3) and β-cat<sup>Δ/Δ</sup> (Δ/Δ1, Δ/Δ2 and Δ/Δ6) mESCs. (C): Western blots of β-catenin and Gapdh in wild-type (NCH4.3 and R1), β-cat<sup>f1/f1</sup> (f1/f12), β-cat<sup>f1/Δ</sup> (f1/Δ2 and f1/Δ3), β-cat<sup>Δ/Δ</sup> (Δ/Δ2, Δ/Δ6 and Δ/Δ8) and β-catenin rescued β-cat<sup>Δ/Δ</sup> mESCs (rsc). (D and E): Immunofluorescence staining for β-catenin (red), α-catenin (green), E-cadherin (red), Oct3/4 (red), Nanog (green) of β-cat<sup>f1/f1</sup> and β-cat<sup>Δ/Δ</sup> mESC colonies as observed under confocal microscopy. Nuclei are stained for DAPI (blue). Scale bars in (D) and (E) are 20 μm.  
doi:10.1371/journal.pone.0063265.g001



**Figure 2. Differentiation potential of embryo-derived β-cat<sup>Δ/Δ</sup> mESCs.** (A): Phase contrast pictures of EBs derived from β-cat<sup>fl/fl</sup> and β-cat<sup>Δ/Δ</sup> mESCs on day 7 of differentiation. Scale bars are 500 μm. (B): Immunofluorescence staining for Afp (green), α-SMA (red) and Tuj-1 (green) of β-cat<sup>fl/fl</sup>, β-cat<sup>Δ/Δ</sup> and β-catenin rescued β-cat<sup>Δ/Δ</sup> mESCs on day 14 of differentiation. Nuclei are stained for DAPI (blue). Scale bars are 200 μm. (C): Expression levels of Sox17 and Brachyury(T) relative to Gapdh in β-cat<sup>fl/fl</sup> (blue bar), β-cat<sup>Δ/Δ</sup> (light blue bar) and β-catenin rescued β-cat<sup>Δ/Δ</sup> (yellow bar) mESCs on day 6 of differentiation. (D): Fluorescence microscopic images of EGFP-β-cat<sup>Δ/Δ</sup> mESC colonies. They constitutively expressed EGFP. Scale bars are 500 μm. (E): Fluorescent stereomicroscopic image of an embryo on E12.5 generated from blastocysts injected with EGFP-β-cat<sup>Δ/Δ</sup> mESCs. The contribution of β-cat<sup>Δ/Δ</sup> mESCs were barely detected anywhere in the whole body. Scale bars are 2 mm. (F): Chimeras generated by injection of β-cat<sup>fl/fl</sup> and β-cat<sup>fl/Δ</sup> mESCs into ICR host blastocysts. Offspring coat color demonstrates high contribution chimeras. doi:10.1371/journal.pone.0063265.g002

**Aberrant *in vivo* Differentiation of β-cat<sup>Δ/Δ</sup> mESCs in Teratoma Assay and Subsequent Development into Germ Cell Tumors**

Wild-type pluripotent ESCs generate benign teratomas composed of well differentiated tissues of endo-, meso- and ectodermal origin. We tested the ability of β-catenin-deficient and β-cat<sup>fl/fl</sup> mESCs to form the three germ layer lineages in teratomas. After

three to five weeks of subcutaneous injection, the tumors which had developed were excised and histologically analyzed. The tumors derived from β-cat<sup>Δ/Δ</sup> mESCs were grossly characterized by areas of hemorrhage and necrosis, which were hardly observed in the teratomas derived from β-cat<sup>fl/fl</sup> mESCs (Figure 3A). All tumors generated from independent β-cat<sup>Δ/Δ</sup> mESC lines showed severe differentiation defects in histological sections (Figure 3B,

middle column) and a grossly undifferentiated cancer-like appearance (Figure 4). Multiple gene expression analysis of teratoma, tumor and F9 embryonal carcinoma (EC) cells by qRT-PCR using a TaqMan Array Mouse Stem Cell Pluripotency Card revealed that teratomas derived from wild-type and res- $\beta$ -cat $^{\Delta/\Delta}$  mESCs were clearly separate from tumors derived from  $\beta$ -cat $^{\Delta/\Delta}$  mESCs and F9 EC cells, whereas the gene expression pattern of undifferentiated wild-type, res- $\beta$ -cat $^{\Delta/\Delta}$  and  $\beta$ -cat $^{\Delta/\Delta}$  mESCs were very similar to each other and differed only from the F9 EC cells (Figure S5B). As subtle differentiation is difficult to recognize using morphological criteria of tumors generated from  $\beta$ -cat $^{\Delta/\Delta}$  mESC lines, we used three differentiation markers to identify the cellular types. Cytokeratin 5/8 and Desmin antibodies did not stain tumor sections of  $\beta$ -cat $^{\Delta/\Delta}$  mESC lines, in contrast to  $\beta$ -cat $^{fl/fl}$  and res- $\beta$ -cat $^{\Delta/\Delta}$  teratomas in which approximately 10–40% of the cells were positively stained (Figure 3B). Also, the neuron-specific nuclear protein marker, Neuronal Nuclei (NeuN) was expressed in the tumor sections of  $\beta$ -cat $^{\Delta/\Delta}$  mESC lines, but at a much lower rate than in the teratomas of  $\beta$ -cat $^{fl/fl}$  and res- $\beta$ -cat $^{\Delta/\Delta}$  (Figure 3B).

Careful observation of numerous tumor sections of different  $\beta$ -cat $^{\Delta/\Delta}$  mESC lines generated independently in separate animals surprisingly revealed pathological carcinomatous features resembling heterogeneous mixtures of germ cell tumors (GCTs) composed of seminoma, embryonal carcinoma, and choriocarcinoma characters (Figure 4). While the well-characterized human germ cell tumors allows identification for histologic classification [24], to date, no animal model is available for analyzing testicular GCT formation and progression [25]. “Seminoma” lesions in  $\beta$ -cat $^{\Delta/\Delta}$  tumors were histologically characterized by a composition of tubular structures lined by seminoma cells with clear cytoplasm, and well-defined cytoplasmic borders, central to marginally located nuclei. These gross appearances were similar to that of classic seminoma in humans in that they had a “fried-egg” appearance (Figure 4). “Embryonal carcinoma (EC)” lesions of the  $\beta$ -cat $^{\Delta/\Delta}$  tumors displayed a papillary pattern, cohesive clustered growth with marked cytologic atypia, and central necrosis of the lesion (Figure 4). “Choriocarcinoma” lesions were easily identified in the  $\beta$ -cat $^{\Delta/\Delta}$  tumor sections by the area of hemorrhage and necrosis both macro- and microscopically. They were characterized by the coexistence of smaller cells with clear cytoplasm and the much larger syncytiotrophoblastic giant cells with huge, pleomorphic nuclei and abundant eosinophilic cytoplasm (Figure 4). Testicular GCTs in human are heterogeneous and contain diverse histopathology and variable clinical course and prognosis [26]. To classify GCTs, immunomarkers are vital. Pluripotent stem cell markers such as OCT3/4, NANOG, and SALL4 are used in clinical trials as they are very sensitive and specific markers [26,27,28]. In our immunohistochemical analysis using specific markers of GCTs, pan-Cytokeratin (AE1/AE3) were focally positive in “EC” lesions and strongly positive in “choriocarcinoma” areas of the  $\beta$ -cat $^{\Delta/\Delta}$  tumors, but not expressed in the “seminoma” areas. OCT3/4 is one of the most robust diagnostic markers of human testicular GCTs [25]. “Seminomas” and “ECs” lesions showed strong positive nuclear staining for Oct3/4, but “choriocarcinoma” cells were negative. SALL4 has been reported to be expressed in subtypes of GCT with high sensitivity and specificity [28,29]. “Seminoma” and “EC” lesions showed positive staining, but “choriocarcinoma” areas of the  $\beta$ -cat $^{\Delta/\Delta}$  tumors were negative. Notably, in all attempts,  $\beta$ -cat $^{\Delta/\Delta}$  mESC lines generated tumors with a carcinomatous appearance, whereas wild-type counterparts gave rise to teratomas with normal differentiation patterns (Figure 5).

We sought to confirm our findings by qRT-PCR for pluripotent markers. Quantitative RT-PCR analysis was performed independently more than three times for each sample.  $\beta$ -cat $^{\Delta/\Delta}$  tumors expressed oct3/4, nanog and lefty1 at high levels (Figure 6A). In contrast, transcript levels of oct3/4, nanog and lefty1 in  $\beta$ -cat $^{fl/fl}$  and res- $\beta$ -cat $^{\Delta/\Delta}$  teratomas were markedly lower than those in  $\beta$ -cat $^{\Delta/\Delta}$  tumors (Figure 6A). In addition, three germ layer differentiation markers of afp, brachyury (I) and neuro D1 were down-regulated in  $\beta$ -cat $^{\Delta/\Delta}$  tumors, while these differentiation markers were clearly detected in  $\beta$ -cat $^{fl/fl}$  and res- $\beta$ -cat $^{\Delta/\Delta}$  teratomas (Figure 6B). Additionally, western blot analysis showed that Nanog and Oct3/4 were detected at the protein level in  $\beta$ -cat $^{\Delta/\Delta}$  tumors, while they were undetected in teratomas generated from  $\beta$ -cat $^{fl/fl}$  mESC lines (Figure 6C).

In the clinical diagnosis of GCTs, most yolk sac tumors produce AFP, but classic seminomas, pure ECs and choriocarcinomas do not [30]. The afp gene was expressed in teratomas induced by  $\beta$ -cat $^{fl/fl}$  and res- $\beta$ -cat $^{\Delta/\Delta}$  mESCs, but not in tumors induced by  $\beta$ -cat $^{\Delta/\Delta}$  mESCs. Lack of afp expression in tumors induced by  $\beta$ -cat $^{\Delta/\Delta}$  mESCs is compatible with the results of the histological analysis in that  $\beta$ -cat $^{\Delta/\Delta}$  tumors did not contain yolk sac elements. Hence, our teratoma assay data strongly suggest that embryo-derived  $\beta$ -cat $^{\Delta/\Delta}$  mESCs transformed into grossly undifferentiated malignant tumors composed of testicular mixed germ cell tumors including classic seminomas, embryonal carcinomas and choriocarcinomas.

#### $\beta$ -cat $^{\Delta/\Delta}$ ESC Properties can be Rescued with a wild-type $\beta$ -catenin

We generated a piggyBac vector carrying a CAG promoter-driven wild-type  $\beta$ -catenin-2A-mCherry for long-term stable expression to restore the differentiation deficiency of  $\beta$ -cat $^{\Delta/\Delta}$  mESCs. We confirmed the establishment of  $\beta$ -catenin- expression in  $\beta$ -cat $^{\Delta/\Delta}$  mESC (res- $\beta$ -cat $^{\Delta/\Delta}$  mESC) by mCherry expression (Figure S4A) and  $\beta$ -catenin protein (Figures 1C, S4B).  $\beta$ -Catenin,  $\alpha$ -catenin and E-cadherin staining and distribution of res- $\beta$ -cat $^{\Delta/\Delta}$  mESCs were similar to  $\beta$ -cat $^{fl/fl}$  mESCs (Figure S4B). The *in vitro* differentiation assay showed that endoderm, mesoderm, and ectoderm differentiation of res- $\beta$ -cat $^{\Delta/\Delta}$  mESCs were restored and were indistinguishable from  $\beta$ -cat $^{fl/fl}$  mESCs (Figure 2B and 3B). In the chimera assay, we readily detected the contribution of res- $\beta$ -cat $^{\Delta/\Delta}$  mESCs in the body at E10.5 (Figure S4C). Together, our rescue experiment results suggest that the re-expression of  $\beta$ -catenin in  $\beta$ -cat $^{\Delta/\Delta}$  mESCs is sufficient to restore them to a wild-type-like mESC identity in *in vitro* and *in vivo*. Furthermore, we sought to analyze whether re-expression of  $\beta$ -catenin can prevent oncogenesis of  $\beta$ -cat $^{\Delta/\Delta}$  mESCs. Histological analysis of res- $\beta$ -cat $^{\Delta/\Delta}$  tumors showed well-differentiated tissues of endo-, meso- and ectodermal origin instead of the undifferentiated carcinomatous appearance of mixed GCTs (Figure 5). The expression pattern of pluripotent and differentiation markers in res- $\beta$ -cat $^{\Delta/\Delta}$  tumors became comparable to that in  $\beta$ -cat $^{fl/fl}$  tumors (Figure 6). Tumors derived from res- $\beta$ -cat $^{\Delta/\Delta}$  mESCs were histopathologically diagnosed as mature teratomas, composed of well multi-differentiated tissues. Thus, embryo-derived  $\beta$ -cat $^{\Delta/\Delta}$  mESCs lost cancerous properties and gained multiple differentiation potential after the restoration of expression of wild  $\beta$ -catenin. Taken together, our rescue data suggest that the restoration of expression of wild-type  $\beta$ -catenin in  $\beta$ -cat $^{\Delta/\Delta}$  mESCs is sufficient to restore the wild-type-like identity of ESCs.

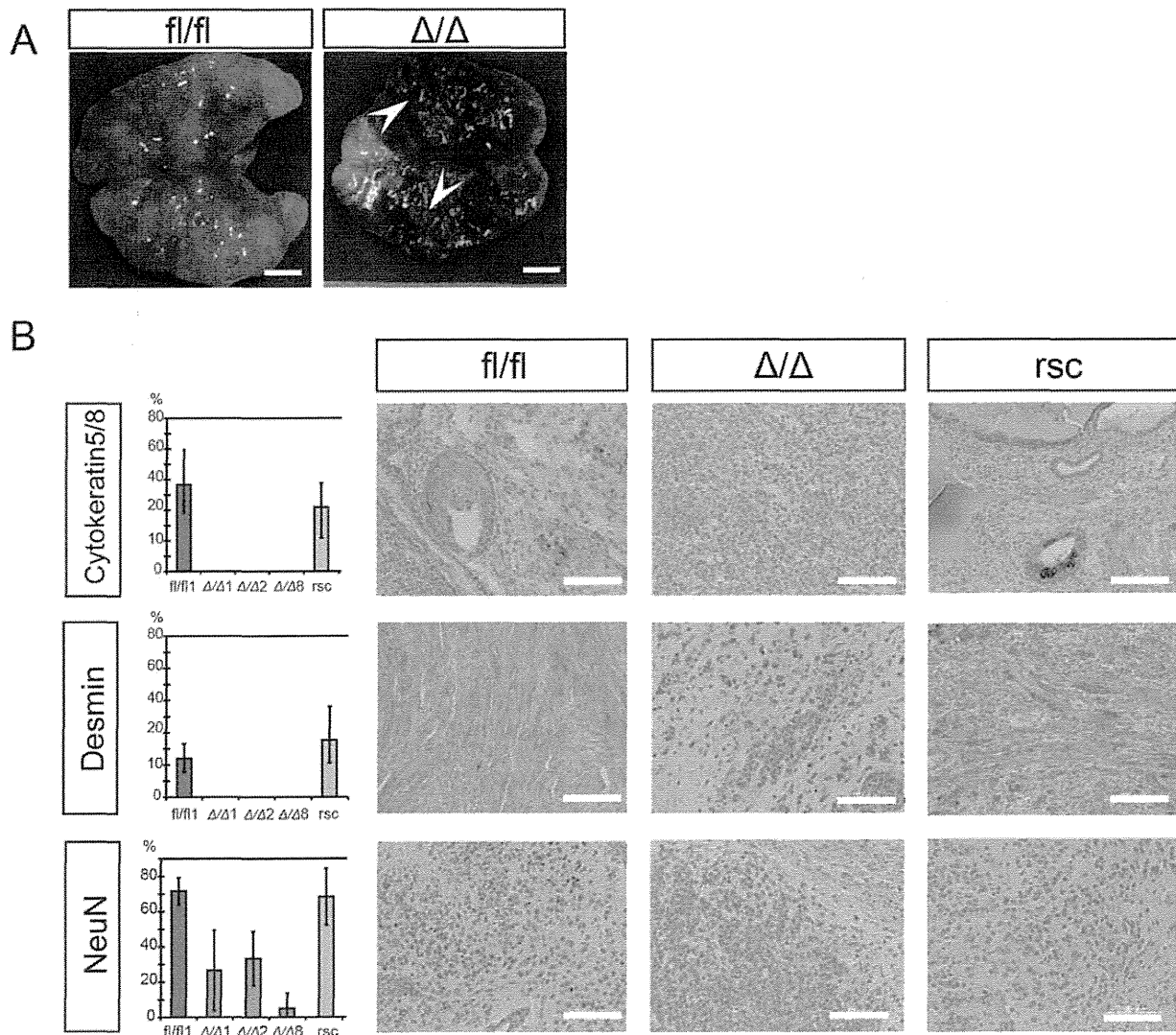


**Figure 3. Immunohistochemical examination of tumors generated from ESCs either β-cat<sup>Δ/Δ</sup> or β-cat<sup>fl/fl</sup>.** (A): The gross image of a tumor mass derived from β-cat<sup>fl/fl</sup> mESC is shown on the left and that of a tumor derived from β-cat<sup>Δ/Δ</sup> mESCs is shown on the right. β-cat<sup>Δ/Δ</sup> tumor mass was characterized by extensive intra-tumoral hemorrhage (white arrow head). Scale bars are 5 mm. (B): Immunohistochemical staining for Cytokeratin 5/8, Desmin and Neuronal nuclear antigen (NeuN) in tumors derived from mESCs of β-cat<sup>fl/fl</sup>, β-cat<sup>Δ/Δ</sup> or res-β-cat<sup>Δ/Δ</sup>. Tissue sections of β-cat<sup>Δ/Δ</sup> tumors displayed high level staining only for the neuronal differentiation marker NeuN, while there was no detectable staining for Cytokeratin 5/8 or Desmin. Tissue sections of both β-cat<sup>fl/fl</sup> and res-β-cat<sup>Δ/Δ</sup> tumors displayed multiple differentiations as shown in three markers' positive staining. The left bar graph shows percentages of Cytokeratin 5/8, Desmin and NeuN positive areas with standard deviation (n=3) as the vertical axis and each tumor as the horizontal axis. Scale bars are 100 μm.  
doi:10.1371/journal.pone.0063265.g003

**Discussion**

Multicellular organisms require stem cells and precise control of them to maintain tissue homeostasis, the replacement of terminally differentiated, aged or damaged cells [31]. Loss of stem cell activity and tissue homeostasis is likely linked to the emergence of diseases including cancer [32,33]. There is considerable interest in finding ways of perpetuating the pluripotency of embryo-derived cells, and gaining this knowledge is of vital importance for many potential biomedical applications related to tissue engineering and disease modeling [31,34]. ESCs are one of the most characterized embryo-derived pluripotent stem cells and Wnt/β-catenin signaling has been implicated in their maintenance for both mouse and

human [35,36]. The ICM of the blastocyst delaminates giving rise to a primitive ectoderm and a primitive endoderm layer, and further differentiated cells progressively lose their differentiation potential. ESCs can be derived from the pluripotent ICM of blastocysts. In addition, β-catenin does not play a crucial role during preimplantation development [37], and at the implantation stage, inactivation of the canonical Wnt/β-catenin signaling pathway blocks blastocyst competency for implantation [38]. It remains unclear whether this signaling is crucial for the acquisition of pluripotency from the ICM of β-catenin-deficient preimplantation embryos.



Type of tumor derived from β-cat<sup>ΔΔ</sup> ESCs

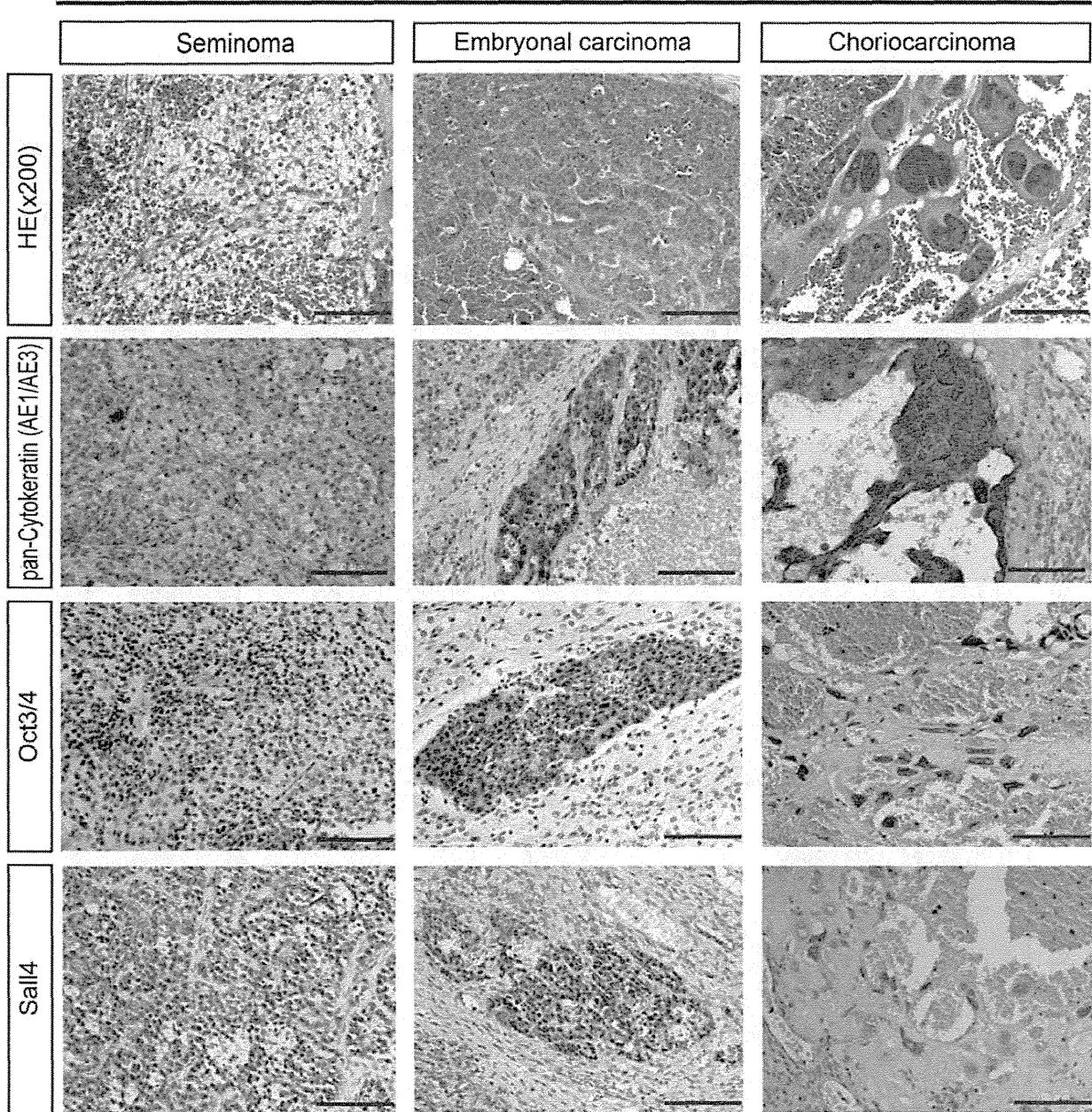


**Figure 4. Histological and immunohistochemical examination of β-cat<sup>ΔΔ</sup> tumors.** Careful examination of numerous tumor sections stained with hematoxylin and eosin (HE) from different β-cat<sup>ΔΔ</sup> mESC lines generated independently in separate animals revealed that each β-cat<sup>ΔΔ</sup> tumor contained three subtypes (seminoma, embryonal carcinoma, choriocarcinoma) of carcinomatous germ cell tumor components. The “seminoma” component is characterized by large uniform dispersed tumor cells displaying clear cytoplasm and distinct cell membrane. Histologic features of the “seminoma” were “fried-egg” appearance: central nucleus with nucleolus, clear cytoplasm and well-defined cell borders. The “embryonal carcinoma (EC)” displayed a papillary pattern, with cohesive clustered growth and marked cytologic atypia. The “choriocarcinoma” was identified by syncytiotrophoblastic giant cells with extensive hemorrhage. The syncytiotrophoblastic giant cells had huge, pleomorphic nuclei and abundant eosinophilic cytoplasm. The “seminoma” displayed very high levels of nuclear OCT4 and Sall4 immunoreactivity, but was negative for pan-cytokeratin. “EC” was strongly positive for pan-cytokeratin, Oct3/4 and Sall4. The syncytiotrophoblastic giant cells of the “choriocarcinoma” showed positive cytoplasmic staining for pan-cytokeratin, but negative nuclear immunostaining for Oct3/4 and Sall4. Scale bars are 100 μm.  
doi:10.1371/journal.pone.0063265.g004

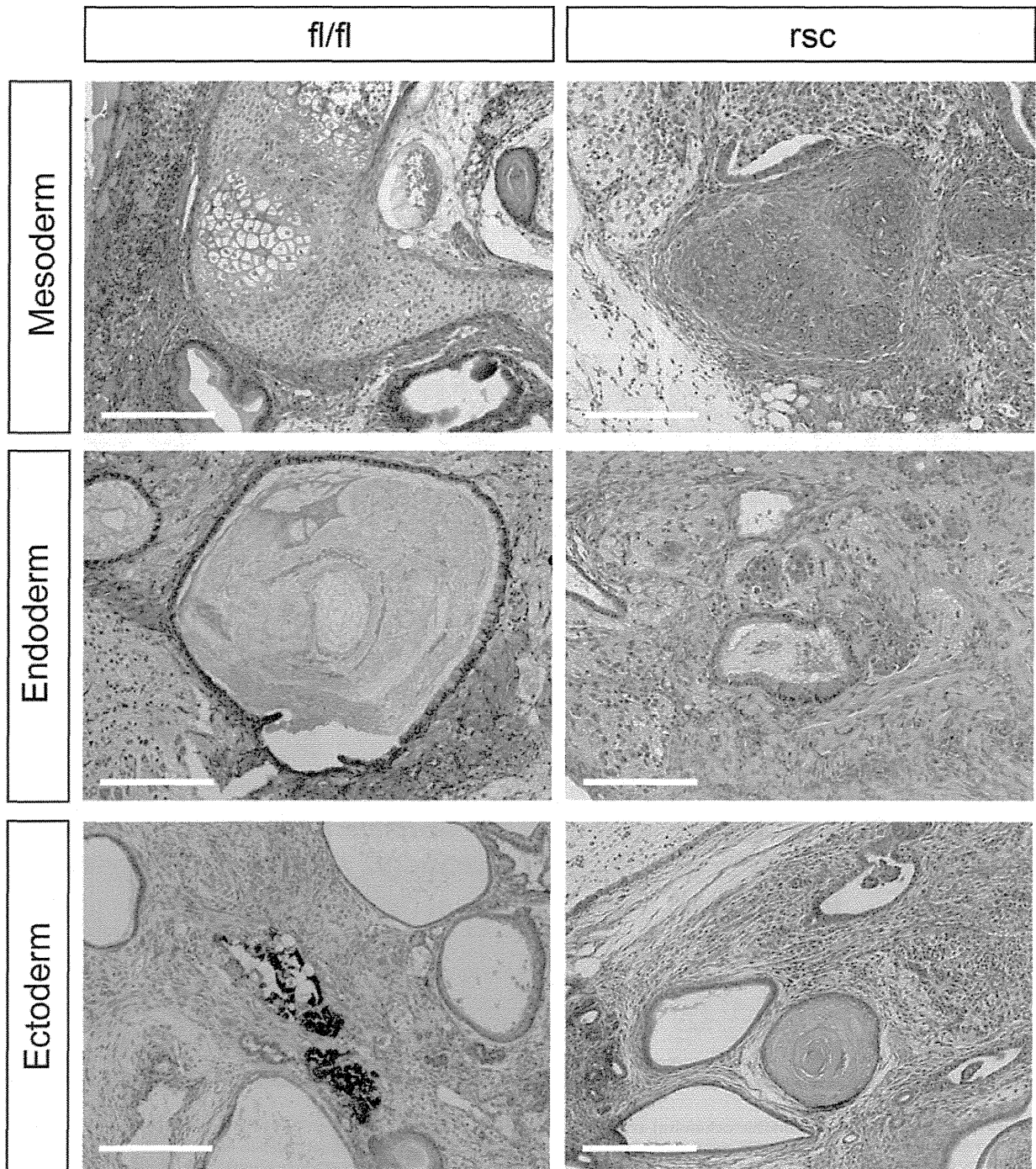
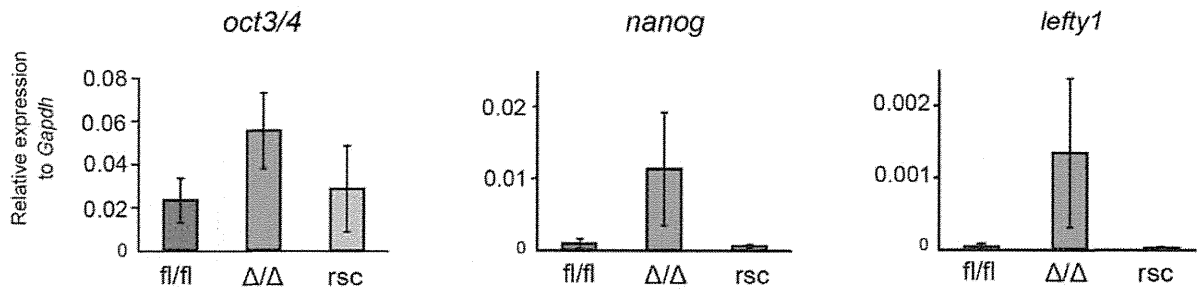
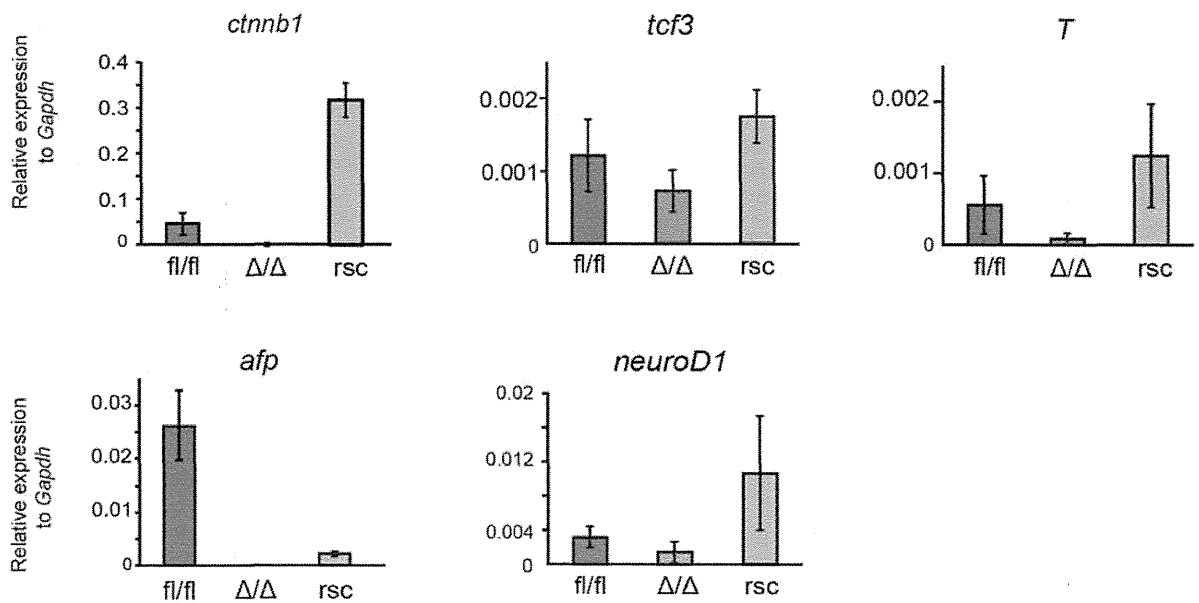


**Figure 5. The histological tumorigenic properties of  $\beta$ -cat <sup>$\Delta/\Delta$</sup>  ESCs can be restored to wild-type ESCs.**  $\beta$ -cat<sup>*fl/fl*</sup> teratomas consisted of well-differentiated mesodermal tissues (bone and cartilage), endodermal tissues (glandular epithelial structures) and ectodermal tissues (pigmented cells).  $\beta$ -catenin-rescued  $\beta$ -cat <sup>$\Delta/\Delta$</sup>  mESCs (res- $\beta$ -cat <sup>$\Delta/\Delta$</sup>  mESCs) gave rise to multilineage differentiated teratoma possessing mesoderm (bone and cartilage), endoderm (glandular epithelial structures) and ectoderm (epidermal tissue). Scale bars are 100  $\mu$ m. doi:10.1371/journal.pone.0063265.g005

A



B



C

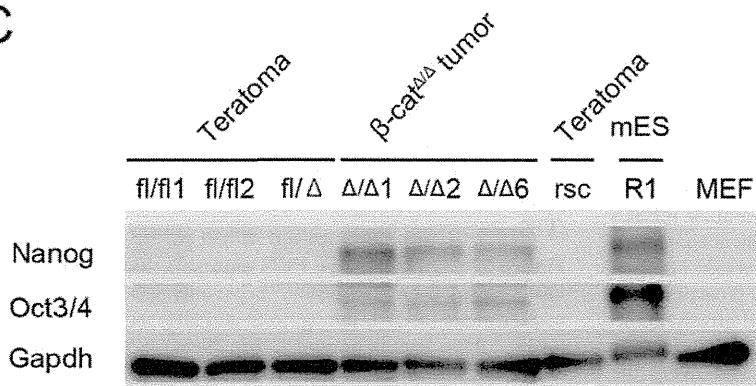


**Figure 6. Quantitative PCR and western blot examination of wild-type ESCs derived teratomas, res-β-cat<sup>Δ/Δ</sup> teratomas and β-cat<sup>Δ/Δ</sup> tumors.** (A and B): Expression levels of self-renewal marker genes (oct3/4, nanog, lefty1) and the downstream genes of Wnt/β-catenin signaling (Ctnnb1, tcf3, T) and early differentiation markers (afp, neuroD1, T) relative to Gapdh in β-cat<sup>fl/fl</sup> (blue bar), res-β-cat<sup>Δ/Δ</sup> (yellow bar) and β-cat<sup>Δ/Δ</sup> (light blue bar) mESC derived teratomas or tumors. (C) Western blots of Nanog, Oct3/4 and Gapdh for teratomas derived from β-cat<sup>fl/fl</sup> (fl/fl1, fl/fl2), β-cat<sup>fl/Δ</sup>, res-β-cat<sup>Δ/Δ</sup> (rsc) and R1 mESCs, tumors derived from β-cat<sup>Δ/Δ</sup> (Δ/Δ1, Δ/Δ2, Δ/Δ6) mESC. MEF was used as a control. Abbreviation: MEF, mouse embryonic fibroblast.  
doi:10.1371/journal.pone.0063265.g006

### Acquisition of Self-renewal Capacity, but Impaired Multilineage Differentiation after ESC Derivation without β-catenin

Previous studies failed to eliminate the effects of remnant β-catenin of maternal or paternal origin. Our conditional mutagenesis studies of β-catenin excluded remnant β-catenin in sperm and eggs, demonstrating that β-catenin is dispensable for fertilized eggs. Furthermore, β-catenin is not required for the acquisition of self-renewal potential by embryo-derived stem cells. However, β-catenin is an indispensable prerequisite for pluripotency. Embryos lacking functional β-catenin activity show a development loss following implantation at around E7.0 with defects in anterior-posterior patterning and mesoderm and definitive endoderm formation [9,21,22]. The role of β-catenin in early development remained to be elucidated because embryonic lethality is associated with the loss-of-function mutation. We observed that the *in vitro* differentiation of embryo-derived β-cat<sup>Δ/Δ</sup> mESCs is impaired similarly to β-catenin-mutant embryos [21,22]. β-Catenin-defect mESCs contribute to chimeric embryos, but the contribution ratio is quite low compared to control mESCs [7]. Previous experiments made observations at earlier times of pregnancy (E7.0 to E8.5). In contrast, our chimeric embryo studies were analyzed on E12.5 and no chimeric compartments were detected. This may have been due to the progressive loss of contribution of β-catenin-defective cells. In other words, β-catenin is required for cellular differentiation and/or viability in early embryogenesis up to E12.5. Notably, the defects of β-cat<sup>Δ/Δ</sup> mESCs in differentiation *in vitro* and *in vivo* could be rescued by re-introducing functional β-catenin. Thus, β-catenin is a caretaker in both *in vitro* ESC differentiation and *in vivo* cellular differentiation during development.

### Implicating Loss-of-function Mutation in β-catenin in Testicular Germ Cell Tumorigenesis

The central player in the canonical Wnt cascade is β-catenin, a cytoplasmic protein whose stability is regulated by the destruction complex. The tumor suppressor protein, Axin acts as the scaffold of this complex as it directly interacts with all other components including β-catenin, the tumor suppressor protein, APC, and the two kinase families CK1 and GSK3 [39]. Deregulated Wnt/β-catenin signaling is associated with many human diseases, including cancer, osteoporosis, aging and degenerative disorders [39,40,41]. Constitutive β-catenin signaling, resulting from deficiency of the destruction complex or oncogenic β-catenin mutations that prevent its degradation, leads to excessive stem cell renewal/proliferation that predisposes cells to tumorigenesis [2,42]. Previously, two groups of researchers independently showed that APC mutant and GSK3α/β double-mutant mESCs remain undifferentiated and possess a malignant phenotype in the teratoma assay [43,44]. APC-mutant mESCs generated undifferentiated carcinomatous tumors with raised levels of β-catenin [43], while GSK3α/β double-mutant mESCs generated grossly undifferentiated carcinomatous tumors with bone tissues as the only differentiated structures [44]. The mechanisms underlying the oncogenesis of both the APC-mutant and GSK3α/β double-mutant mESCs is unclear. Our β-catenin loss-of-function mESCs

displayed a tumorigenic phenotype with the carcinomatous appearance of mixed germ cell tumors in a teratoma assay. The tumors derived from our embryo-derived β-cat<sup>Δ/Δ</sup> mESCs included a mixture of classic seminomas, embryonal carcinomas and choriocarcinomas, identifications we made based on the histological features of human carcinomas [24,26]. All examined tumors of β-cat<sup>Δ/Δ</sup> mESCs consistently expressed the pluripotency markers Oct4, Nanog and Lefty1, while β-cat<sup>fl/fl</sup> mESCs failed to maintain expression of these markers. We successfully rescued the multilineage differentiation potential of β-cat<sup>Δ/Δ</sup> mESCs by restoring the expression of functional β-catenin. Loss of β-Catenin can still maintain self-renewal of mESCs and sustain pluripotency markers such as Nanog and Oct3/4. The failure in repression of pluripotential genes might correlate with formation of germ cell tumor in β-cat<sup>Δ/Δ</sup> mESCs. To our knowledge, no animal model enables us to study tumorigenesis of mixed germ cell tumors. Human germ cell tumors are a heterogeneous type of neoplasm, mostly originate from germ cells [27]. The characteristics of germ cell tumors are either derived from the process of tumorigenesis or a reflection of normal embryonal development, a feature which contributes to the complexity of these tumors [25]. Embryo-derived pluripotent stem cells allow a better understanding of the biology of GCTs.

Our results reveal that β-catenin signaling guides healthy development and normal cellular differentiation, and disruption of β-catenin signaling initiates oncogenicity turning embryo-derived stem cells into mixed germ cell tumors. The re-introduction of β-catenin expression can rescue the normal pluripotency, highlighting potential clinical approaches for clinical treatments of mixed germ cell tumors. There is currently no animal model of testicular mixed germ cell tumors [25]. Therefore, β-cat<sup>Δ/Δ</sup> mESCs are novel research tools for the study of tumorigenesis of testicular germ cell tumors and the function of β-catenin in cell-fate switching between tissue homeostasis and oncogenesis.

### Supporting Information

**Figure S1 Growth curve, western blotting and chromosome analysis of embryo-derived β-cat<sup>Δ/Δ</sup> mESCs.** (A): The examined β-cat<sup>Δ/Δ</sup> mESC lines had normal karyotypes. The β-cat<sup>Δ/Δ</sup> (Δ/Δ2) mESC line showed a normal karyotype of 40XX. (B): Western blots of Nanog and Oct3/4 in wild-type (NCH4.3 and R1), β-cat<sup>fl/fl</sup> (fl/fl2), β-cat<sup>fl/Δ</sup> (fl/Δ2 and fl/Δ3), β-cat<sup>Δ/Δ</sup> (Δ/Δ2, Δ/Δ6 and Δ/Δ8) mESCs and MEF. (C): Growth curve of β-cat<sup>fl/fl</sup> (fl/fl2), β-cat<sup>fl/Δ</sup> (fl/Δ3), β-cat<sup>Δ/Δ</sup> (Δ/Δ6 and Δ/Δ8) and res-β-cat<sup>Δ/Δ</sup> (rsc) mESC lines over a period of 5 days in feeder-free and serum-free culture (2i+LIF). Cell population doublings are plotted against days (n = 3, SD). (TIF)

**Figure S2 Quantitative PCR examination of β-cat<sup>fl/fl</sup>, β-cat<sup>fl/Δ</sup> and β-cat<sup>Δ/Δ</sup> ESCs.** Expression levels of self-renewal marker genes (oct3/4, nanog, sox2 and klf4) relative to Gapdh in β-cat<sup>fl/fl</sup> (blue bar: fl/fl1 and fl/fl2), β-cat<sup>fl/Δ</sup> (purple bar: fl/Δ2 and fl/Δ3) and β-cat<sup>Δ/Δ</sup> (light blue bar: Δ/Δ1, Δ/Δ2 and Δ/Δ8) mESCs. (TIF)

**Figure S3 β-cat<sup>Δ/Δ</sup> ESCs in serum- and feeder-free conditions of culture.** (A): Phase-contrast images of cellular expansion of β-cat<sup>fl/fl</sup> and β-cat<sup>Δ/Δ</sup> mESCs under serum- and feeder-free conditions using the 2i+LIF system with mitogen-activated protein kinase kinase (MEK) inhibitor (PD0325901) and GSK3β inhibitor (CHIR99021) on days 1, 3 and 5. Scale bars are 200 μm. (B): Quantitative PCR analysis of β-cat<sup>fl/fl</sup> (fl/fl1 and fl/fl2) and β-cat<sup>Δ/Δ</sup> (Δ/Δ1 and Δ/Δ2) mESCs in serum- and feeder-free conditions. Axin2 expression was normalized to Gapdh. In the canonical Wnt/β-catenin signaling cascade, Axin2 acts as the scaffold of the β-catenin destruction complex. Axin2 was not up-regulated in our β-cat<sup>Δ/Δ</sup> mESCs, and so β-cat<sup>Δ/Δ</sup> mESCs are transcriptionally defective in the canonical Wnt/β-catenin pathway. (TIF)

**Figure S4 β-catenin-rescued β-cat<sup>Δ/Δ</sup> ESCs showed restored development potential in the chimera assay.** (A): β-cat<sup>Δ/Δ</sup> mESCs with an integrated piggyBac vector carrying a CAG promoter-driven β-catenin-2A-mCherry (res-β-cat<sup>Δ/Δ</sup> mESCs) expressed red fluorescent protein mCherry. Scale bars are 500 μm. (B): Immunofluorescence staining for β-catenin (red), α-catenin (green), and E-cadherin (green) of res-β-cat<sup>Δ/Δ</sup> mESC colonies as observed under confocal microscopy. Nuclei are stained for DAPI (blue). Scale bars are 20 μm. (C): Chimeras were generated by injection of res-β-cat<sup>Δ/Δ</sup> mESCs into ICR host blastocysts. Chimeric embryos on E10.5 displayed the high contribution of res-β-cat<sup>Δ/Δ</sup> mESCs to the whole body. Scale bars are 500 μm. (TIF)

**Figure S5 Hierarchical clustering analysis of expression data from the TaqMan array across the 96 marker genes.** Multiple gene expression analysis of mESC lines and F9 (A) and tumors (B) by quantitative PCR using TaqMan Array Mouse Stem Cell Pluripotency Card (Life technologies). (A): The two subtypes of stem cell lines were clustered into distinct clusters with reversed gene expression patterns. The group of wild-type, res-β-cat<sup>Δ/Δ</sup> and β-cat<sup>Δ/Δ</sup> mESC lines was clustered from F9 EC. (B): Tumor clustering was different from stem cells. β-cat<sup>Δ/Δ</sup>

tumors were clustered into the same cluster as tumors derived from F9 EC, and separately clustered from teratomas of wild-type and res-β-cat<sup>Δ/Δ</sup> mESCs. The level of expression of each gene in each sample, relative to the median level of expression of that gene across all the samples, is represented using a red-black-green color scale as shown in the key (green: below median; black: equal to median; red: above median). (TIF)

**Figure S6 Chimeric embryos at E12.5 generated from EGFP-β-cat<sup>Δ/Δ</sup> mESCs.** Contribution of EGFP-β-cat<sup>Δ/Δ</sup> mESCs to mouse embryonic development. Embryos were analyzed using a uorescence stereomicroscope on E12.5. Embryos with scattered EGFP fluorescence showed limb malformations (white arrow head). Scale bars are 2 mm. (TIF)

**Figure S7 Immunofluorescence staining of Plakoglobin in β-cat<sup>fl/fl</sup>, β-cat<sup>Δ/Δ</sup> and res-β-cat<sup>Δ/Δ</sup>.** Immunofluorescence staining for Plakoglobin (green) and DAPI (blue) of β-cat<sup>fl/fl</sup>, β-cat<sup>Δ/Δ</sup> and res-β-cat<sup>Δ/Δ</sup> mESC colony as observed under confocal microscopy. Scale bars are 20 μm. (TIF)

### Acknowledgments

We are grateful to Hideki Tsumura and staff of the Animal Care Facility at NRICHD for mouse husbandry. We thank Shoko Sato for blastocyst injections and dissection embryos, Seiya Kanai and Kahori Minami for technical assistance, and Tomoyuki Kawasaki for help with editing the figures. We also thank Wataru Nishie for providing antibody. The authors would like to thank Yusuke Marikawa and Kevin Eggan for critical reading of the manuscript and helpful discussion and members of the Umezawa laboratory for suggestions.

### Author Contributions

Conceived and designed the experiments: NO HA TH JI. Performed the experiments: NO TS TM YT AH KY MY. Analyzed the data: NO HA TS TM JI MY TH NK KM YY AU. Contributed reagents/materials/analysis tools: MY TH NK YY. Wrote the paper: NO HA.

### References

- Marikawa Y (2006) Wnt/β-catenin signaling and body plan formation in mouse embryos. *Semin Cell Dev Biol* 17: 175–184.
- MacDonald BT, Tamai K, He X (2009) Wnt/β-catenin signaling: Components, Mechanisms, and Diseases. *Dev Cell* 17: 9–26.
- Evans MJ, Kaufman MH (1981) Establishment in culture of pluripotential cells from mouse embryos. *Nature* 292: 154–156.
- Thomson JA, Itskovitz-Eldor J, Shapiro SS, Waknitz MA, Swiergiel JJ, et al. (1998) Embryonic stem cell lines derived from human blastocysts. *Science* 282: 1145–1147.
- Sokol SY (2011) Maintaining embryonic stem cell pluripotency with Wnt signaling. *Development* 138: 4341–4350.
- Grigoryan T, Wend P, Klaus A, Birchmeier W (2008) Deciphering the function of canonical Wnt signals in development and disease: conditional loss- and gain-of-function mutations of beta-catenin in mice. *Genes Dev* 22: 2308–2341.
- Lyashenko N, Winter M, Migliorini D, Biechele T, Moon RT, et al. (2011) Differential requirement for the dual functions of β-catenin in embryonic stem cell self-renewal and germ layer formation. *Nat Cell Biol* 13: 753–761.
- Wray J, Kalkan T, Gomez-Lopez S, Eckardt D, Cook A, et al. (2011) Inhibition of glycogen synthase kinase-3 alleviates Tcf3 repression of the pluripotency network and increases embryonic stem cell resistance to differentiation. *Nat Cell Biol* 13: 838–845.
- Takezawa Y, Yoshida K, Miyado K, Sato M, Nakamura A, et al. (2011) β-catenin is a molecular switch that regulates transition of cell-cell adhesion to fusion. *Sci Rep* 1: 68.
- Brault V, Moore R, Kutsch S, Ishibashi M, Rowitch DH, et al. (2001) Inactivation of the beta-catenin gene by Wnt1-Cre-mediated deletion results in dramatic brain malformation and failure of craniofacial development. *Development* 128: 1253–1264.
- Matsumura H, Hasuwa H, Inoue N, Ikawa M, Okabe M (2004) Lineage-specific cell disruption in living mice by Cre-mediated expression of diphtheria toxin A chain. *Biochem Biophys Res Commun* 321: 275–279.
- Di Giorgio FP, Carrasco MA, Siao MC, Maniatis T, Eggen K (2007) Non-cell autonomous effect of glia on motor neurons in an embryonic stem cell-based ALS model. *Nat Neurosci* 10: 608–614.
- Ying QL, Wray J, Nichols J, Battle-Morera L, Doble B, et al. (2008) The ground state of embryonic stem cell self-renewal. *Nature* 453: 519–523.
- Silva J, Barrandon O, Nichols J, Kawaguchi J, Theunissen TW, Smith A (2008) Promotion of reprogramming to ground state pluripotency by signal inhibition. *PLoS Biol* 6: e253.
- Akutsu H, Miura T, Machida M, Birumachi J, Hamada A, et al. (2009) Maintenance of pluripotency and self-renewal ability of mouse embryonic stem cells in the absence of tetraspanin CD9. *Differentiation* 78: 137–142.
- Nagy A, Rossant J, Nagy R, Abramow-Newerly W, Roder JC (1993) Derivation of completely cell-culture derived mice from early-passage embryonic stem cells. *Proc Natl Acad Sci USA* 90: 8424–8428.
- Yusa K, Rad R, Takeda J, Bradley A (2009) Generation of transgene-free induced pluripotent mouse stem cells by the *piggyBac* transposon. *Nat Methods* 6: 363–369.
- Ishii R, Kami D, Toyoda M, Makino H, Gojo S, et al. (2012) Placenta to Cartilage: Direct conversion of human placenta to chondrocytes with transformation by defined factors. *Mol Biol Cell* 23: 3511–3521.
- Ikawa M, Yamada S, Nakanishi T, Okabe M (1999) Green fluorescent protein (GFP) as a vital marker in mammals. *Curr Top Dev Biol* 44: 1–20.
- Stadtfed M, Apostolou E, Akutsu H, Fukuda A, Follett P, et al. (2010) Aberrant silencing of imprinted genes on chromosome 12qF1 in mouse induced stem cell. *Nature* 465: 175–181.



21. Haegel H, Larue L, Ohsugi M, Fedorov L, Herrenknecht K, et al. (1995) Lack of beta-catenin affects mouse development at gastrulation. *Development* 121: 3529–3537.
22. Huelsken J, Vogel R, Brinkmann V, Erdmann B, Birchmeier C, et al. (2000) Requirement for beta-catenin in anterior-posterior axis formation in mice. *J Cell Biol* 148: 567–578.
23. Arnold SJ, Stappert J, Bauer A, Kispert A, Herrmann BG, et al. (2000) Brachyury is a target gene of the Wnt/beta-catenin signaling pathway. *Mech Dev* 91: 249–258.
24. Eble JN, Sauter G, Epstein JI, Sesterhenn IA (2004) Pathology and genetics of tumours of the urinary system and male genital organs. Lyon, France: IARC Press: 218–249. World Health Organization Classification of Tumours.
25. Oosterhuis JW, Looijenga LH (2005) Testicular germ-cell tumours in a broader perspective. *Nat Rev Cancer* 5: 210–222.
26. Bahrami A, Ro JY, Ayala AG (2007) An overview of testicular germ cell tumors. *Arch Pathol Lab Med* 131: 1267–1279.
27. Talerman A (1985) Germ cell tumours. *Ann Pathol* 5: 145–157.
28. Cao D, Humphrey PA, Allan RW (2009) SALL4 is a novel sensitive and specific marker for metastatic germ cell tumors, with particular utility in detection of metastatic yolk sac tumors. *Cancer* 115: 2640–2651.
29. Cao D, Li J, Guo CC, Allan RW, Humphrey PA (2009) SALL4 is a novel diagnostic marker for testicular germ cell tumors. *Am J Surg Pathol* 33: 1065–1077.
30. Talerman A, Haije WG, Baggerman L (1980) Serum alphafetoprotein (AFP) in patients with germ cell tumors of the gonads and extragonadal sites: correlation between endodermal sinus (yolk sac) tumor and raised serum AFP. *Cancer* 46: 380–385.
31. Boiani M, Scholer HR (2005) Regulatory networks in embryo-derived pluripotent stem cells. *Nat Rev Mol Cell Biol* 6: 872–884.
32. Beachy PA, Karhadkar SS, Berman DM (2004) Tissue repair and stem cell renewal in carcinogenesis. *Nature* 432: 324–331.
33. Laird DJ, von Andrian UH, Wagers AJ (2008) Stem cell trafficking in tissue development, growth, and disease. *Cell* 132: 612–630.
34. Murry CE, Keller G (2008) Differentiation of embryonic stem cells to clinically relevant populations: lessons from embryonic development. *Cell* 132: 661–680.
35. Niwa H (2007) How is pluripotency determined and maintained? *Development* 134: 635–646.
36. Davidson KC, Adams AM, Goodson JM, McDonald CE, Potter JC, et al. (2012) Wnt/ $\beta$ -catenin signaling promotes differentiation, not self-renewal, of human embryonic stem cells and is repressed by Oct4. *Proc Natl Acad Sci U S A* 109: 4485–4490.
37. DeVries WN, Evsikov AV, Haac BE, Fancher KS, Holbrook AE, et al. (2004) Maternal beta-catenin and E-cadherin in mouse development. *Development* 131: 4435–4445.
38. Xie H, Tranguch S, Jia X, Zhang H, Das SK, et al. (2008) Inactivation of nuclear Wnt- $\beta$ -catenin signaling limits blastocyst competency for implantation. *Development* 135: 717–727.
39. Clevers H (2006) Wnt/ $\beta$ -catenin signaling in development and disease. *Cell* 127: 469–480.
40. Moon RT, Kohn AD, De Ferrari GV, Kaykas A (2004) WNT and beta-catenin signalling: diseases and therapies. *Nat Rev Genet* 5: 691–701.
41. Clevers H, Nusse R (2012) Wnt/ $\beta$ -catenin Signaling and Disease. *Cell* 149: 1192–1205.
42. Reya T, Clevers H (2005) Wnt signaling in stem cells and cancer. *Nature* 434: 843–850.
43. Kielman MF, Rindapää M, Gaspar C, van Poppel N, Breukel C, et al. (2002) Apc modulates embryonic stem-cell differentiation by controlling the dosage of beta-catenin signaling. *Nat Genet* 32: 594–605.
44. Doble BW, Patel S, Wood GA, Kockeritz LK, Woodgett JR (2007) Functional redundancy of GSK-3 $\alpha$  and GSK-3 $\beta$  in Wnt/ $\beta$ -catenin signaling shown by using an allelic series of embryonic stem cell lines. *Dev Cell* 12: 957–971.



## Physical Cues of Biomaterials Guide Stem Cell Differentiation Fate

Akon Higuchi,<sup>\*,†,‡,§</sup> Qing-Dong Ling,<sup>§,||</sup> Yung Chang,<sup>⊥</sup> Shih-Tien Hsu,<sup>▽</sup> and Akihiro Umezawa<sup>‡</sup>

<sup>†</sup>Department of Chemical and Materials Engineering, National Central University, Jhongli, Taoyuan 32001, Taiwan

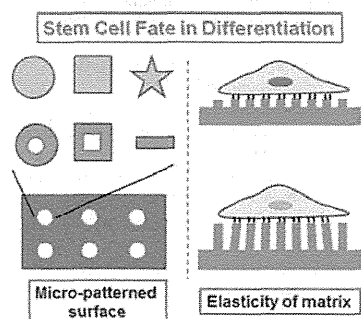
<sup>‡</sup>Department of Reproductive Biology, National Research Institute for Child Health and Development, 2-10-1 Okura, Setagaya-ku, Tokyo 157-8535, Japan

<sup>§</sup>Cathay Medical Research Institute, Cathay General Hospital, No. 32, Ln 160, Jian-Cheng Road, Hsi-Chi City, Taipei 221, Taiwan

<sup>||</sup>Institute of Systems Biology and Bioinformatics, National Central University, No. 300 Jhongda Rd., Jhongli, Taoyuan 32001, Taiwan

<sup>⊥</sup>Department of Chemical Engineering, R&D Center for Membrane Technology, Chung Yuan Christian University, 200 Chung-Bei Rd., Jhongli, Taoyuan 320, Taiwan

<sup>▽</sup>Taiwan Landseed Hospital, 77 Kuangtai Road, Pingjen City, Tao-Yuan County 32405, Taiwan



### CONTENTS

1. Introduction	3297
2. Effect of Elasticity of Cell Culture Materials on Stem Cell Differentiation	3298
2.1. Elasticity of Substrate Directs Stem Cell Differentiation Fate in 2-D Culture	3299
2.2. Pluripotent Maintenance of ESCs, iPSCs, and MSCs on Soft Culture Substrate	3304
2.3. Mechanism of Regulation of Stem Cell Differentiation Fate by ECM and Substrate Elasticity in 2-D Culture	3305
2.4. Elasticity of Substrate Directs Stem Cell Differentiation Fate in 3-D Culture	3306
2.5. Results Contradictory to Engler's Research in 2-D Culture	3307
2.6. Results Contradictory to Engler's Research in 3-D Culture	3308
3. Effect of Topography of Cell Culture Materials on Stem Cell Differentiation	3309
3.1. Preparation of Micro- and Nanopatterned Surfaces	3309
3.2. Adipogenic and Osteogenic Stem Cell Differentiation on Micropatterned Surfaces	3311
3.3. Chondrogenic, Myogenic, and Hepatic Stem Cell Differentiation on Micropatterned Surfaces	3314
3.4. Neural Stem Cell Differentiation on Micro-patterned Surfaces	3315
3.5. Stem Cell Differentiation on Nanofiber Surfaces	3316

3.5.1. Stem Cell Differentiation on Nanofibers Formed by Self-Assembly of Amphiphile Peptides	3316
3.5.2. Stem Cell Differentiation on Nanofibers Prepared by Electrospinning	3318
3.5.3. Stem Cell Differentiation on Nanofibers Prepared Using Phase Separation	3322
4. Conclusion	3323
Author Information	3323
Corresponding Author	3323
Notes	3323
Biographies	3323
Acknowledgments	3324
References	3325

### 1. INTRODUCTION

Millions of people lose or damage their organs or tissues due to disease, birth defects, or accidents each year. Stem cells, such as embryonic stem cells (ESCs), induced pluripotent stem cells (iPSCs), adult stem cells, and fetal stem cells are an attractive prospect for regenerative medicine and tissue engineering.<sup>1–3</sup> ESCs derived from preimplantation embryos have the potential to differentiate into any cell type derived from the three germ layers: the ectoderm (nerves and epidermal tissues), mesoderm (bone, muscle, and blood), and endoderm (lungs, liver, gastrointestinal tract, and pancreas).<sup>2–7</sup> iPSCs are known to have similar properties to ESCs, including the expression of certain pluripotent stem cell genes and proteins and differentiability into many types of cells derived from the three germ layers.<sup>8–12</sup>

The pluripotent nature of ESCs and iPSCs opens many avenues for potential stem cell-based regenerative therapies and the development of drug discovery platforms.<sup>2,3,5,13</sup> The nearest-term therapeutic use of ESCs and iPSCs may be in the treatment of disorders of single cell types, such as the transplantation of differentiated nerve cells (TH<sup>+</sup> cells, dopamine-secreting cells) for the treatment of Parkinson's disease or  $\beta$  cells (insulin-secreting cells) for the treatment of diabetes.<sup>2,3,13</sup> However, it is difficult to guide iPSCs and ESCs

Received: October 27, 2012

Published: February 7, 2013

to be differentiated into specific lineages of cells due to their pluripotent ability of differentiation.<sup>14–24</sup>

Adult and fetal stem cells can be isolated from a variety of somatic tissues, that is, bone marrow, umbilical cord blood, umbilical cord tissue, amniotic fluid, dental pulp, and other tissues such as fat.<sup>16–22</sup> There have been no reports to date of mesenchymal stem cells (MSCs) or fetal stem cells differentiating into tumors, such as have been reported in ESCs and iPSCs. MSCs are currently the most widely available autologous source of stem cells for practical and clinical applications. However, adult and fetal stem cells have aging problems and limited passage numbers.<sup>25–28</sup>

Stem cell characteristics, such as proper differentiation and maintenance of pluripotency, are regulated not only by the stem cells themselves but also by the microenvironment.<sup>2,3,29</sup> Therefore, mimicking stem cell microenvironments and niches using biopolymers (biomaterials) could facilitate the production of large numbers of stem cells and specifically differentiated cells needed for *in vitro* regenerative medicine.

Biological cues, such as growth factors, hormones, small chemicals, and extracellular matrix, can decide the stem cell fates of differentiation and pluripotency.<sup>30,31</sup> Therefore, many research efforts have been chiefly devoted to identifying soluble differentiation factors to mimic the stem cell microenvironment. However, investigators have begun to evaluate the potential importance of physical cues influencing stem cells, such as cell shape, stiffness of cell culture substrates, mechanical forces (e.g., shear stress of culture medium), external forces (e.g., electrical force, magnetic force), and light signaling.<sup>18,32–44</sup> Some excellent reviews and original articles addressing biomaterials guiding stem cell differentiation are listed in Table 1.<sup>2,3,19,20,22,32,36,40,41,45–55</sup> However, few review articles have specifically addressed the physical cues of cell culture biomaterials for stem cell differentiation, and the review articles that have been written do not describe the methods and results in comprehensive detail for chemists and materials scientists.<sup>33,36,37,40,47,52,56,57</sup> Therefore, this review focuses on physical cues of biomaterials guiding the differentiation of MSCs, ESCs, and iPSCs into several lineages, such as adipocytes, chondrocytes, osteoblasts, muscle cells, endothelial cells, and neural cells. We do not focus on the differentiation of stem cells triggered by mechanical<sup>33,36–38</sup> and external forces<sup>18,36,37,47</sup> in this review because these effects are not directly related to the biomaterials used in stem cell culture. The physical cues of biomaterials in stem cell culture described in this review are classified as biomaterial (a) elasticity and (b) topography. Recently, not only biological cues such as growth factors and bioactive molecules, but also physical cues of biomaterials such as elasticity and topography are considered to be important factors for stem cell differentiation into specific lineages. This is because small and large biomolecules that induce differentiation of stem cells have been highly investigated. Nowadays, it is difficult to find novel biomolecules for differentiation of stem cells and to find much higher efficiency of stem cell differentiation into desired lineages solely by combination of these biomolecules in culture medium. Biomaterials for stem cell culture are focused as a tool for fine-tuning of stem cell differentiation, because it is quite recent for researchers to realize biomaterials can guide stem cell fate of differentiation. For example, the morphology of stem cells can be regulated by elasticity and topography of cell culture biomaterials, which indicates that the elasticity and topography of the biomaterials can regulate signal transduction of stem cells

**Table 1. Some Key Review and Original Articles Addressing Biomaterials Guiding Stem Cell Differentiation**

author	contents	ref (year)
Lee and Mooney	hydrogels for tissue engineering	45 (2001)
Engler et al.	matrix elasticity directs stem cell lineage	32 (2006)
Benoit et al.	small functional groups for controlled differentiation of hydrogel-encapsulated hMSCs	20 (2008)
Liao et al.	stem cells and biomimetic materials strategies for tissue Engineering	55 (2008)
Wescocoe et al.	biochemical and biophysical environment in chondrogenic stem cell differentiation	40 (2008)
Little et al.	biomaterials for neural stem cell microenvironments	46 (2008)
Dellatore et al.	mimicking stem cell niches to increase stem cell expansion	47 (2008)
Boskey and Roy	cell culture systems for studies of bone and tooth mineralization	48 (2008)
Burdick and Vunjak-Novakovic	engineered microenvironments for controlled stem cell differentiation	41 (2009)
Guilak et al.	control of stem cell fate by physical interactions with ECM	36 (2009)
Mei et al.	combinatorial development of biomaterials for clonal growth of human pluripotent stem cells	49 (2010)
Melkounian et al.	synthetic peptide-acrylate surfaces for long-term self-renewal of hESCs	50 (2010)
Gilbert et al.	substrate elasticity regulates skeletal muscle stem cell self-renewal	51 (2010)
Huebsch et al.	harnessing traction-mediated manipulation of the cell/matrix interface to control stem-cell fate	19 (2010)
Ghfar-Zadeh et al.	stem cell microenvironment for cardiac tissue regeneration	52 (2011)
Balakrishnam and Benerjee	biopolymer-based hydrogels for cartilage tissue engineering	53 (2011)
Higuchi et al.	biomaterials for the feeder-free culture of hESCs and human iPSCs	2 (2011)
Kim et al.	design of artificial extracellular matrices for tissue engineering	54 (2011)
Higuchi et al.	biomimetic cell culture proteins for stem cell differentiation	3 (2012)
Trappmann et al.	ECM tethering regulates stem-cell fate	22 (2012)

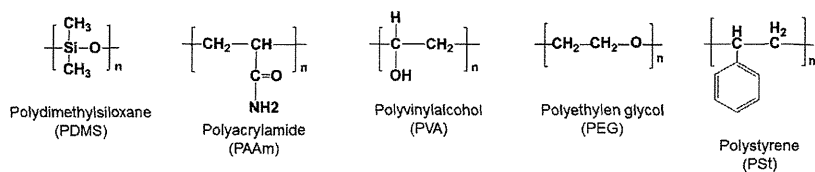
and subsequently guide stem cell differentiation into specific lineages.

These effects are described in detail in the following sections. The chemical schematics of the biomaterials described in this review are summarized in Figure 1. Some of the genes and proteins mentioned in this review that are typically utilized to verify the differentiation of stem cells into specific lineages and their descriptions are summarized in Table 2.<sup>2,3,19,32,35,58–84</sup> Various staining methods used to characterize specific lineages are summarized in Table 3.<sup>2,3,18,19,22,32,51,64,85–87</sup>

## 2. EFFECT OF ELASTICITY OF CELL CULTURE MATERIALS ON STEM CELL DIFFERENTIATION

Diverse microenvironmental factors contribute to overall stem cell fate (i.e., differentiation into specific lineages). In particular, physical interactions between cells and the elasticity (or rigidity and stiffness) of the extracellular matrix (ECM) where they are cultured can influence stem cell fate, although the control of stem cell fate has been classically attributed to genetic or molecular mediators.<sup>36,88</sup> Recently, many researchers have begun to realize that the elasticity of cell culture substrates

## (a) Synthetic polymer



## (b) Biopolymer

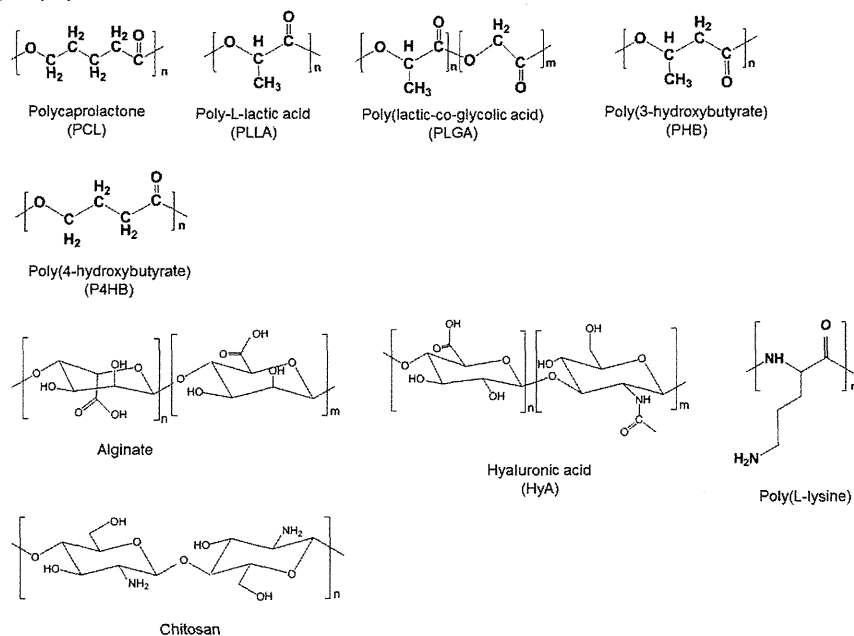


**Figure 1.** Chemical schematics of synthetic polymers (polydimethylsiloxane [PDMS], polyacrylamide [PAAm], poly(vinyl alcohol) [PVA], poly(ethylene glycol) [PEG], and polystyrene [PSt]) (a) and biopolymers (poly( $\epsilon$ -caprolactone) [PCL], poly(L-lactic acid) [PLLA], poly(lactic-co-glycolic acid) [PLGA], poly(3-hydroxybutyrate) [PHB], poly(4-hydroxybutyrate) [P4HB], alginate, hyaluronic acid [HyA], poly(L-lysine), and chitosan) (b) used as substrates, hydrogels, and scaffolds for the proliferation and differentiation of stem cells.

defines the lineage commitment of human MSCs (hMSCs). Stem cells tend to efficiently differentiate into specific tissue lineages when they are cultured on biomaterials with similar elasticity to those tissues. Figure 2 provides examples of the elasticity of various human tissues and synthetic and natural polymers derived from the literature.<sup>32,49,77,87,89–92</sup>

The elasticity of cell culture substrates can clearly influence cell morphology, cell phenotype, and focal adhesions, especially in two-dimensional (2-D) culture.<sup>51,58,62,66,72–75,86,88,93,94</sup> Mechanosensing of substrates by stem cells is considered to be generated by integrin-mediated focal adhesion signaling.<sup>34</sup> Integrins are receptors mediating the attachment between cells and ECM in cell culture substrates or tissues. They are composed of obligate heterodimers containing two distinct chains of  $\alpha$  and  $\beta$  subunits. Integrins contribute to cell-matrix signaling by activating intracellular tyrosine kinase and phosphatase signaling to elicit downstream biochemical signals important for the regulation of gene expression and stem cell fate.<sup>89</sup>

Previous studies have suggested that nonmuscle myosin IIA (NMMIIA)-dependent contractility of the actin cytoskeleton is an important mediator of the mechanosensing and mechano-transduction processes in different types of stem cells.<sup>32,34,89,95–97</sup> Furthermore, the elasticity of cell culture

substrates affects intracellular signaling through mechanotransducers such as Rho kinase (ROCK) and focal adhesion kinase (FAK) and subsequently regulates the differentiation lineages of stem cells in 2-D culture.<sup>74</sup> Here, we review the effect of substrate elasticity (or rigidity) on the differentiation lineages of stem cells in 2-D and three-dimensional (3-D) culture. Tables 4 and 5 show examples from the literature of the effects of substrate elasticity on the differentiation of stem cells in 2-D and 3-D culture, respectively (refs 16, 19, 21, 22, 32, 58, 59, 62–66, 70, 73–75, 77, 85–87, 93, 94, 98–114).

### 2.1. Elasticity of Substrate Directs Stem Cell Differentiation Fate in 2-D Culture

Engler et al. cultured hMSCs on polyacrylamide (PAAm) substrates (hydrogels) of different stiffness coated with collagen type I in expansion medium (i.e., culture medium containing no differentiation-inducing biochemical factors).<sup>32</sup> Figure 3 shows the proteins and transcription profiles reported by Engler et al. of neuronal markers (P-NFH and  $\beta$ -III tubulin, Table 2), a muscle transcription factor (MyD1), and an osteoblast transcription factor (Runx2) expressed in hMSCs cultured on substrates with varying stiffness.<sup>32</sup> Several other proteins and transcription factors expressed in MSCs cultured on substrates with varying stiffness investigated by other research-

Table 2. Genes and Proteins To Investigate the Differentiation of Stem Cells into Specific Lineages

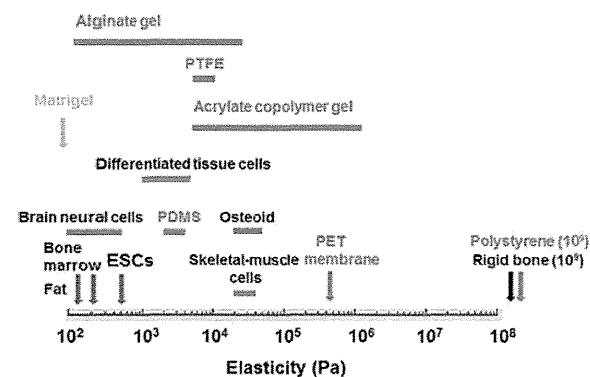
differentiation lineage	gene or protein	specification	ref (example)	differentiation lineage	gene or protein	specification	ref (example)				
osteoblasts	Runx2 (CBF $\alpha$ 1)	early osteoblast marker	19, 32, 66	muscle	myocardin	smooth muscle cell marker	67				
	osterix	early osteoblast marker	3		smoothelin	smooth muscle cell marker	67				
	osteocalcin (OCN)	late osteoblast marker	32, 59, 61		collagen type 4	myogenic marker	69				
	osteopontin (OPN, Spp1)	late osteoblast marker	58, 61		desmin	myogenic marker	69				
	alkaline phosphatase (ALP)	early osteoblast marker	61		Pax3	myogenic marker	32, 69				
	bone sialoprotein (BSP)	osteoblast marker	78, 79		Pax7	myogenic marker	32, 69				
	collagen type I (Col I)	osteoblast marker	74		myogenin (MYOG)	myogenic marker	69				
chondrocytes	Sox 9	chondrocyte marker	35, 63, 67	neural cells	MyoD, MyoD1	myogenic marker	69				
	Col2A1	chondrocyte marker	67		nestin	neural stem/progenitor cell marker	71, 72, 77				
	aggrecan (ACAN)	chondrocyte marker	80		ENO2	neural cell	59				
	collagen type II (Col II)	chondrocyte marker	64		$\beta$ -tubulin III or $\beta$ -III tubulin (Tuj-1)	neuronal marker	32, 66, 68				
	collagen type X (Col X)	chondrocyte marker	3		tyrosine hydroxylase (TH)	neuronal marker (dopamin secreting cells)	71				
	cartilage oligomeric protein (COMP)	chondrocyte marker	80		neurofilament light chain (NEFL, NFL)	neuronal marker	71–73				
						neurofilament heavy chain (NFH)	neuronal marker	32, 73			
adipocytes	adipocyte lipid-binding protein (ALBP)	adipocyte marker	3	microtubule-associated protein 2 (MAP2)	mature neuronal marker	72, 76					
	PPAR $\gamma$	adipocyte marker	35		glial fibrillary acidic protein (GFAP)	astrocyte marker	62, 68				
	aP-2	adipocyte marker	81		galactosylceramidase (GalC)	oligodendrocyte marker	71				
	lipoprotein lipase (LPL)	adipocyte marker	75		RIP	mature oligodendrocyte	71				
cardiomyocytes	cardiac troponin T (cTnT)	cardiomyocyte marker	3, 84	O4	oligodendrocyte marker	68					
	desmin	cardiomyocyte marker	82, 83		CNPase	oligodendrocyte marker	76				
	myosin heavy chain (MHC)	cardiomyocyte marker	84			Flk-1	endothelial cell marker	70			
	myosin light chain (MLC)	cardiomyocyte marker	84				$\alpha$ -fetoprotein (AFP)	early hepatocytes	65		
	Nkx2.5	cardiomyocyte marker	84					albumin (ALB)	mature hepatocytes	65	
	GATA-4	cardiomyocyte marker	84						Epithelial cell adhesion molecule (EpcAM)	hepatic stem cells, hepatoblasts	65
										neural cell adhesion molecule (NCAM)	hepatic stem cells (and neural cells)
			E-cadherin (CDH1)	hepatic stem cells (and ESCs, iPSCs)							65
				ESC, iPSCs	Oct3/4						pluripotent marker
					Sox2	pluripotent marker					2
					Nanog	pluripotent marker	2				
muscle	smooth muscle $\alpha$ -actin (SMA)	smooth muscle cell marker			70						
	$\alpha$ -actin	smooth muscle cell marker			60						
	calponin 1	smooth muscle (contractile) marker			59, 67						

ers<sup>62,63,66,70,75</sup> are also included in Figure 3. Softer materials, with similar stiffness to the brain at approximately 0.3 kPa, tend to cause cells to express neuronal morphologies and neural markers (P-NFH,  $\beta$ -III tubulin), whereas stiffer materials of approximately 10 kPa mimicking muscle guide hMSCs and tend to cause cells to express myogenic markers (MyoD) in Engler's study.<sup>32</sup> Rigid materials similar to collagenous bone induced the expression of osteogenic marker Runx2 at a stiffness of approximately 35 kPa.<sup>32</sup> The myoblast cell line C2C12 also exhibited substrate stiffness-dependent MyoD

expression, where the highest expression of MyoD was found in C2C12 cells cultured on substrate with a stiffness of approximately 10 kPa, although the expression intensity of MyoD in the myoblast cell line was twice as high as in hMSCs. Similarly, the highest expression of osteogenic marker Runx2 was found in the osteoblast cell line hFOB cultured on substrate with a stiffness of approximately 35 kPa, with an expression intensity 1.5 times greater than that in hMSCs.<sup>32</sup> Stiff substrates promote focal adhesion growth and elongation. Focal adhesions provide hMSCs with force transmission

**Table 3. Staining Method To Investigate the Differentiation of Stem Cells into Specific Lineages**

staining method	detection site	characterization	ref (example)
paxillin labeling	paxillin	focal adhesion	32
phalloidin F-actin	F-actin	focal adhesion	22, 19, 85
vinculin	focal adhesion protein	focal adhesion	22, 86
oil red O	oil droplet	adipocytes	87
nile red	oil droplet	adipocytes	3
alizarin red	calcium	osteoblasts	85, 87
von Kossa	calcium phosphate	osteoblasts	18
alkali phosphatase	alkali phosphatase activity	osteoblasts	86
safranin-O	proteoglycan	chondrocytes	64
alcian blue	proteoglycan	chondrocytes	3
toluidine blue	proteoglycan	chondrocytes	86
DAPI	DNA	nucleus	19
Hoechst	DNA	nucleus	51
Masson'S trichrome	tissue	connective tissue, nuclei, cytoplasm	64
hematoxylin and eosin (H&E)	tissue	connective tissue, nuclei, cytoplasm	2

**Figure 2.** Examples of the elasticity of human tissues (blue bars and arrows), synthetic polymers (red bars and arrows), and natural polymers (green arrows).

pathways through which to influence their microenvironment via actin–myosin contractions. Therefore, stiffer culture substrates generate stiffer, more highly tensed cells. Cells alter their nonmuscle myosin expression to generate greater forces on the actin cytoskeleton, a necessary step to deform a stiffer matrix.<sup>32</sup> The forces generated on the actin cytoskeleton have been postulated to influence stem cell differentiation. Therefore, stem cells have different differentiation fates when they are cultured on different cell culture substrates.<sup>3–88</sup>

Several researchers have also reported that the stiffness of the cell culture substrate (matrix) is an important factor in the differentiation of stem cells in 2-D culture (refs 16, 34, 51, 58, 62, 66, 72–75, 85, 86, 88, 93, 94, 99, and 100).

The muscle microenvironment enables freshly isolated muscle stem cells to contribute to skeletal muscle regeneration when transplanted in animals. However, muscle stem cells cultured on conventional tissue culture plates lose their “stemness” easily, yielding progenitors with reduced regenerative potential.<sup>51</sup> Gilbert et al. investigated whether the elastic modulus of culture dishes plays a crucial role in muscle stem

cell self-renewal and function in muscle regeneration.<sup>51</sup> They prepared cross-linked poly(ethylene glycol) (PEG) hydrogels with different stiffness values of 2, 12, and 42 kPa on plastic dishes (1  $\mu\text{m}$  thick). Because laminin is a component of the native muscle stem cell niche, it was grafted onto the PEG hydrogels. Under time-lapse observation, the shortening velocity of muscle stem cells was found to decrease on soft PEG hydrogels (99  $\mu\text{m}/\text{h}$ ) compared with those cultured on stiff plastic culture dishes (120  $\mu\text{m}/\text{h}$ ).<sup>51</sup> The total number of muscle stem cells cultured on stiff plastic culture dishes did not change during 1 week of culture because cell division was offset by cell death. However, the number of muscle stem cells cultured on soft PEG hydrogels doubled compared with the cells cultured on rigid plastic culture dishes.<sup>51</sup> This result indicates that muscle stem cell culture on soft PEG hydrogels can augment cell survival. Muscle stem cells cultured on soft PEG hydrogels expressed only 1/3 as much of the myogenic transcription factor myogenin, which indicates differentiation of muscle stem cells, as those cultured on stiff plastic culture dishes after 1 week of culture.<sup>51</sup> It has been demonstrated that soft substrates seem to increase cell numbers by enhancing cell viability and by preventing the differentiation of muscle stem cells in vitro. The function of muscle stem cells cultured on stiff and soft culture substrates was also assessed in vivo to verify that muscle stem cells cultured on soft PEG hydrogels retain their stemness.<sup>51</sup> In vivo functional assays indicated that culturing muscle stem cells on PEG hydrogels matching the physiological modulus (12 kPa) of muscle tissue best preserved their stemness (pluripotency). Muscle stem cells cultured on PEG hydrogels with an elasticity of 12 kPa were retained in mice after 30 days of transplantation, whereas markedly reduced engraftment was observed for muscle stem cells cultured on stiff plastic culture dishes.<sup>51</sup> Mice transplanted with muscle stem cells cultured on soft PEG hydrogels developed new myofibers resulting from regeneration. A transplantation assay of muscle stem cells cultured on various substrates in mice demonstrated that soft PEG hydrogel, but not stiff plastic culture dishes, guided the self-renewal of muscle stem cells.<sup>51</sup>

Healy et al. developed an interfacial hydrogel prepared by creating an interpenetrating polymer network with an oligopeptide containing RGD (arginine-glycine-aspartic acid) sequences on the surface with stiffness values ranging from 10 to 10 000 Pa (Figure 4).<sup>62</sup> Rat neural stem cells proliferated when cultured in serum-free media on the RGD peptide-modified interpenetrating network hydrogels with elastic moduli greater than 100 Pa. The highest expression of neural marker  $\beta$ -III tubulin (Table 2) in rat neural stem cells was observed on the RGD peptide-modified interpenetrating network hydrogels with elastic moduli of 500 Pa, near the physiological stiffness of brain tissue.<sup>62</sup> It was found that neuronal differentiation was favored on softer RGD peptide-modified interpenetrating network hydrogels under mixed glial and neuronal differentiation medium, whereas glial differentiation was favored on stiffer RGD peptide-modified interpenetrating network hydrogels in the same medium. Furthermore, cell spreading, self-renewal, and differentiation were inhibited on the RGD peptide-modified interpenetrating network hydrogels with elastic moduli of approximately 10 Pa.<sup>62</sup> This study demonstrates that physical (elasticity of the cell culture biomaterials) and biochemical (RGD peptide and soluble biochemical factors) factors can regulate the self-renewal and specific differentiation lineages of rat neural stem cells.

**Table 4. Some Research Studies for Differentiation of Stem Cells Cultured on Biomaterials Having Different Elasticity in 2-D Culture<sup>a</sup>**

stem cell source	materials for stem cell culture having different stiffness	differentiation	medium	ref (year)
hMSCs	HyA–gelatin–PEG hydrogels	proliferation and secretion of cytokines	expansion medium	103 (2009)
hMSCs	PAAm gel coated with collagen type I	proliferation and cell morphology	expansion medium	21 (2010)
murine ESC (OGR1)	PAAm gel coated with collagen type I and rigid dishes coated with collagen type I	proliferation with pluripotency	expansion medium	94 (2010)
hMSCs	patterned cross-linked methacrylated HyA gel containing RGDS	proliferation and cell morphology	expansion medium	111 (2010)
murine ESCs (CGR8)	polyion complex nanofilm composed of PLL and HyA	proliferation and cell morphology	expansion medium	104 (2010)
hESCs (H1, H9)	PDMS micropost treated by oxygen plasma	proliferation with pluripotency	expansion medium	105 (2012)
hMSCs	thiol-modified HyA gels and PAAm coated with collagen type I	proliferation and cell morphology	expansion medium	98 (2012)
mESCs (TG2 $\alpha$ E14)	PDMS coated with collagen type I	proliferation, osteoblast, and mesendoderm differentiation	expansion and differentiation medium	58 (2009)
rat MSCs	PDMS grafted with poly(acrylic acid)	osteoblast	differentiation medium	99 (2009)
hMSCs	PAAm gel coated with collagen type I	osteoblast	differentiation medium	74 (2011)
hMSCs	gelatin–hydroxyphenylpropionic acid–tyramine gels cross-linked with HRP and H <sub>2</sub> O <sub>2</sub>	osteoblast	unknown	112 (2012)
umbilical cord MSCs (Wharton's jelly)	PAAm gel grafted with Collagen type I	osteoblast	differentiation medium	16 (2012)
rat MSCs	PDMS coated with fibronectin and gelatin	osteoblast	differentiation medium	85 (2012)
hMSCs (Stro-1 enriched cells)	polyalkyl acrylate coated with fibronectin	osteoblast	expansion medium	113 (2012)
hMSCs	PAAm gel coated with collagen type I and fibronectin	osteoblast, adipocyte	differentiation medium	87 (2009)
human epidermal stem cells, hMSCs	PDMS and PAAm gel grafted with collagen type I	osteoblast, adipocyte	mixed differentiation medium of osteoblast and adipocyte	22 (2012)
hMSCs	PEG gel immobilized fibronectin	osteoblast, adipocyte, neural cell	differentiation medium	114 (2011)
human placenta-derived MSCs, hADSCs	layer-by-layer polyion complex of cationic PLL and anionic HyA	osteoblast, adipocyte, chondrocyte	differentiation medium	86 (2009)
murine embryonic mesenchymal progenitor cells (C3H10T1/2) MSCs	PCL nanofibers and PCL-PES nanofiber by electrospinning method	osteoblast, chondrocyte	differentiation medium	106 (2011)
MSCs	PAAm gel coated with collagen type I	osteoblast, myocyte, and neuron	expansion medium	32 (2006)
hMSCs	PAAm gel grafted with polytrimethylphosphate, polyallylamine, poly(acrylic acid), or collagen type I	osteoblast, myocyte, neuron	expansion and differentiation medium	66 (2011)
murine cardiac progenitor cells, MSCs	PLLA, PCL, PLGA film	cardiomyocyte	differentiation medium	107 (2008)
hMSCs	PAAm gel grafted with collagen I	adipocyte, chondrocyte, smooth muscle cell, schwann cell	expansion and differentiation medium	75 (2011)
hMSCs	PAAm gel grafted with collagen I	myocyte, neural cell	expansion medium	93 (2011)
hMSCs	gelatin–hydroxyphenylpropionic acid gel cross-linked with HRP and H <sub>2</sub> O <sub>2</sub>	myocyte, neuron	expansion medium	73 (2010)
rat NSCs	RGD conjugated PEG-PAAm interpenetrating network gel	neuron and astrocytes	differentiation medium	62 (2008)
embryonic cortices	xyloglucan gel grafted with poly(D-lysine)	neuron	differentiation medium	110 (2009)
rat NSCs	polymethacrylamide–chitosan gel coated with laminin	neuron, oligodendrocyte, astrocyte	differentiation medium	108 (2009)
bovine limbal stem cells	collagen type I gel coated with laminin	limbal epithelial cell	expansion medium	100 (2012)
murine ESCs (ESD3)	fibrin gel	endoderm cell	differentiation medium	109 (2012)

<sup>a</sup>ESC, embryonic stem cells; MSC, mesenchymal stem cells; hMSCs, human MSCs; hADSCs, human adipose-derived stem cells; NSCs, neural stem cells; HyA, hyaluronic acid; PAAm, polyacrylamide; PDMS, polydimethylsiloxane; PES, polyethersulfone; PEG, poly(ethylene glycol); PLL, poly(L-lysine); PLLA, poly(L-lactic acid); PCL, poly( $\epsilon$ -caprolactone); HRP, horse radish peroxidase.

Cell culture substrates with elastic modulus gradients (or storage modulus) are sophisticated materials used to systematically study stem cell differentiation guided by substrate stiffness. Several methods for the preparation of substrates with elastic modulus gradients have been developed and are shown in Figure 5. A monomer solution including a cross-linker is placed under a temperature gradient<sup>85</sup> (Figure 5a) or UV light<sup>93</sup> (Figure 5b), creating a gradient of cross-linking degrees and elastic moduli in the resulting substrate.

Tse and Engler created cross-linked PAAm hydrogels with radial elastic modulus gradients (1 kPa/mm) with a range of 1 to 14 kPa using photopolymerization under a gradient-patterned photomask.<sup>93</sup> It was found that hMSCs in the expansion medium migrated to the stiffer matrix and then differentiated into a more contractile myogenic phenotype on the cross-linked hydrogels grafted with collagen type I, whereas hMSCs expressing the neuronal marker  $\beta$ -III tubulin remained on soft regions of the gradient hydrogels.<sup>93</sup> Several studies suggest that soft cell culture materials guide MSCs into



Table 5. Some Research Studies for Differentiation of Stem Cells Cultured on Biomaterials Having Different Elasticity in 3-D Culture<sup>a</sup>

stem cell source	materials for stem cell culture having different stiffness	differentiation	medium	ref (year)
hMSCs	PAAm gel coated with collagen type I	proliferation and cell morphology	expansion medium	21 (2010)
hMSCs	thiol-modified HyA gels and PAAm coated with collagen type I	proliferation and cell morphology	expansion medium	98 (2012)
rat MSCs	gelatin- $\beta$ tricalcium phosphate sponge	osteoblast	differentiation medium	101 (2005)
hMSCs	PAAm gel coated with collagen type I and fibronectin	osteoblast, adipocyte	differentiation medium	87 (2009)
hMSCs	RGD-modified alginate gel	osteoblast, adipocyte	mixed differentiation medium of osteoblast and adipocyte	19 (2010)
rat MSCs	collagen-glycosaminoglycan scaffold	osteoblasts, chondrocytes	expansion medium	63 (2012)
hMSCs	thiotrophic gel composed of PEG-silica and RGD-alginate gel	osteoblast, myocyte, and neural cell,	expansion medium	59 (2010)
goat MSCs	tyramine-HyA gel cross-linked with HRP and H <sub>2</sub> O <sub>2</sub>	chondrocytes	differentiation medium	64 (2012)
murine cardiac progenitor cells, MSCs	PLLA, PCL, PLGA having hexagonal or square grid geometry	cardiomyocyte	differentiation medium	107 (2008)
rat MSCs	PEG nanofiber coated with collagen type I	smooth muscle cell, endothelial cell	expansion medium	70 (2012)
embryonic cortices	xyloglucan gel grafted with poly(D-lysine)	neuron	differentiation medium	110 (2009)
rat NSCs	alginate hydrogels	neuron	expansion medium	77 (2009)
human fetal liver stem cells	thiol-HyA-PEG gels	endoderm stem/progenitor cells	expansion medium	65 (2011)
hESCs	PLLA, PLGA, PCL coated with matrigel	mesoderm, endoderm, and ectoderm cell	differentiation medium	102 (2011)
murine ESCs (ESD3)	fibrin gel	endoderm cells	differentiation medium	109 (2012)

<sup>a</sup>ESCs, embryonic stem cells; hESCs, human ESCs; MSCs, mesenchymal stem cells; hMSCs, human MSCs; NSCs, neural stem cells; PAAm, polyacrylamide; HyA, hyaluronic acid; PEG, poly(ethylene glycol); PLLA, poly(L-lactic acid), PCL, poly( $\epsilon$ -caprolactone); PLGA; poly(lactic acid-co-glycolic acid).

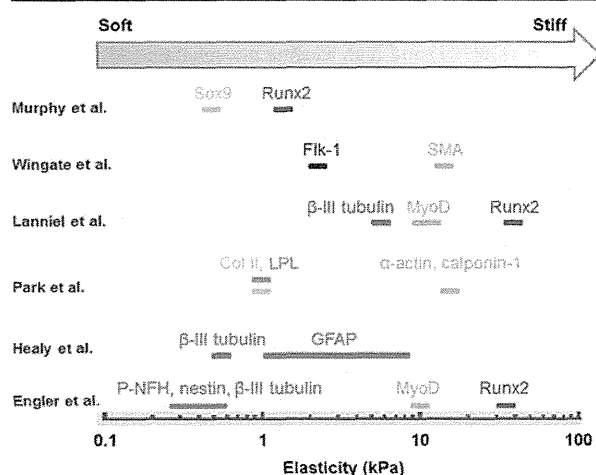


Figure 3. Proteins and transcription profiles of neural markers (red bar; nestin, P-NFH, and  $\beta$ -III tubulin), chondrocyte markers (yellow bar; collagen type II and Sox9), an adipocyte marker (orange bar; LPL), muscle transcription factors (green bar; MyD,  $\alpha$ -actin, calponin-1, and SMA), an osteoblast transcription factor (blue bar; Runx2), and an endothelial marker (dark blue bar; Flk-1) expressed in MSCs cultured on substrates of varied stiffness, as reported by Murphy et al.,<sup>63</sup> Wingate et al.,<sup>70</sup> Lanniel et al.,<sup>66</sup> Park et al.,<sup>75</sup> Healy et al.,<sup>62</sup> and Engler et al.<sup>32</sup>

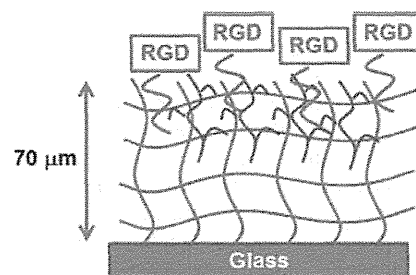
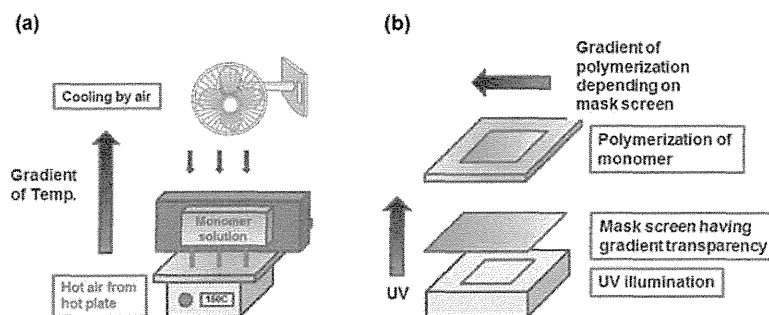


Figure 4. Schematic model developed by Healy et al. of an interpenetrating polymer network with oligopeptides containing surface RGD sequences with different stiffnesses. Modified with permission from ref 62. Copyright 2008 Elsevier Inc.

neuronal differentiation when MSCs are cultured in either expansion medium containing no induction factors or differentiation (induction) medium.<sup>32,59,62,66,72,73,77</sup>

Transforming growth factor  $\beta$  (TGF- $\beta$ ) is known to promote MSC differentiation into either smooth muscle cells or chondrogenic cells. Therefore, Park et al. investigated whether the elasticity of the cell culture substrate affected the differentiation of hMSCs by culturing them on collagen type I gel (soft substrate), collagen-coated culture dishes (stiff substrate), and cross-linked PAAm hydrogels with varying stiffness (1, 3, and 15 kPa) grafted with collagen type I.<sup>75</sup> Cells cultured on soft substrates had less spreading, fewer stress fibers, and lower proliferation rates than hMSCs cultured on



**Figure 5.** Preparation methods of substrates with elastic modulus gradients by monomer polymerization, shown by temperature gradient (a) or intensity of UV light (b). Modified with permission from ref 85 with Copyright 2012 Elsevier Inc. (a) and from ref 93 under a Creative Commons Attribution License (b).

stiff culture substrates. Additionally, hMSCs on stiff substrates displayed higher expression of smooth muscle cell markers ( $\alpha$ -actin and calponin-1) in expansion medium, whereas hMSCs on soft substrates displayed increases in expression of the chondrogenic marker collagen type II and an adipogenic marker (lipoprotein lipase, LPL) (Figure 3).<sup>75</sup> The addition of TGF- $\beta$  in the culture medium promoted the expression of smooth muscle cell markers and suppressed the expression of adipogenic markers on soft culture substrates. However, hMSCs were capable of differentiating into adipocytes on soft culture substrate when they were cultured in adipogenic differentiation medium.<sup>75</sup>

Lanniel et al. investigated differentiation lineages of hMSCs cultured on cross-linked PAAm hydrogels with varying elasticity (stiffness) and functional groups (trimethylphosphate, allylamine, and acrylic acid). Vinyl monomer was polymerized on the surface of the hydrogels using the plasma polymerization method. Cells were cultured on the hydrogels to evaluate the effect of different combinations of physical (substrate elasticity) and chemical cues (several functional groups) on hMSC differentiation.<sup>66</sup> The expression of the osteogenic marker Runx2 was highest in hMSCs cultured in expansion medium without added differentiation (induction) factors on PAAm hydrogels coated with phosphate polymer and with a stiffness of 41 kPa. The myogenic phenotype marker MyoD1 was most highly expressed in hMSCs cultured on PAAm hydrogels coated with poly(acrylic acid) with intermediate stiffness (10–17 kPa) (Figure 3).<sup>66</sup> Neurogenic differentiation as measured by  $\beta$ -III tubulin expression was highest on the softest hydrogels (6.5 kPa) coated with poly(acrylic acid) (Figure 3). Bone nodule formation and matrix calcification were observed on PAAm hydrogels stiffer than 10 kPa that had been coated with polyallylamine in osteogenic induction medium but not on hydrogels coated with collagen type I.<sup>66</sup> These results indicate that hMSC differentiation lineage can be regulated not only by the elasticity (stiffness) of cell culture substrates but also by surface chemistry (different types of functional groups) and differentiation induction factors.

## 2.2. Pluripotent Maintenance of ESCs, iPSCs, and MSCs on Soft Culture Substrate

It is important to maintain ESCs and iPSCs in an undifferentiated state in culture. However, several studies have suggested that undifferentiated ESC cultures actually contain heterogeneous populations identified by the fluctuating expression of various transcripts and cell-surface markers.<sup>94,115–117</sup> One of the major challenges in the field is

to develop optimal culture conditions and culture substrates to maintain the self-renewal and pluripotency of ESCs and iPSCs.

Chowdhury et al. reported that mouse ESCs (mESCs) could maintain pluripotency (as measured by the expression of high levels of pluripotent genes and proteins (Oct3/4, Nanog) and by the generation of homogeneous undifferentiated colonies) when they were cultured in the absence of exogenous leukemia inhibitory factor (LIF) on soft substrates (0.6 kPa) matching the intrinsic stiffness of mESCs, while mESCs could not maintain their self-renewal and pluripotency on conventional stiff culture polystyrene dishes (>4 MPa) coated with collagen type I or on hydrogels with much stiffer moduli.<sup>94</sup> In general, it is necessary to add LIF to the culture medium during the culture and expansion of mESCs to maintain their self-renewal and pluripotency.<sup>2</sup>

However, in this study, several mESC cell lines were able to be cultured on soft substrates without the addition of LIF to the culture medium, maintaining the generation of homogeneous undifferentiated colonies with high expression of pluripotent markers (Oct3/4) and high alkaline phosphatase (ALP) activity (index of pluripotency, see Table 2) up to 15 passages, suggesting that these soft hydrogels could be used for long-term culture of mESCs.<sup>94</sup> It should be noted that laminin and vitronectin are more suitable proteins than collagen, which was used for their study, for ECM immobilized in the cell culture substrate for the maintenance of self-renewal and pluripotency of ESCs and iPSCs.<sup>2</sup> Therefore, it is interesting that mESCs can be cultured on soft hydrogels coated with collagen type I while keeping their self-renewal and pluripotency for 15 passages in the absence of LIF in the culture medium.<sup>94</sup> mESC colonies on soft cell substrates in culture medium without LIF generated low cell-matrix traction and had low stiffness. Both traction and stiffness of the colonies increased with increasing cell culture substrate stiffness, which was also accompanied by down-regulated expression of the pluripotent protein Oct3/4. This suggests that the self-renewal and pluripotency of mESCs can be maintained on soft cell culture substrates via the biophysical mechanism of facilitating the generation of low cell-matrix traction.<sup>94</sup>

However, there is a contradictory report that stiff (rigid) substrates can support the maintenance of hESC pluripotency.<sup>105</sup> Sun et al. macrofabricated elastomeric PDMS micropost arrays in which the height of the PDMS microposts controls substrate stiffness (elasticity) (Figure 6).<sup>105</sup> It is known that PDMS micropost arrays affect cell morphology, focal adhesions, cytoskeleton contractility, and stem cell differentiation.<sup>105,118,119</sup> Human ESCs were cultured on oxygen

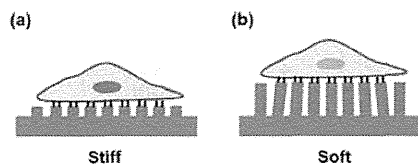


**Figure 6.** Elastomeric PDMS micropost arrays where the height of PDMS microposts control substrate stiffness (elasticity). Short and long microposts lead to stiff and soft surfaces, respectively, although both micropost arrays are prepared with the same components and cross-linking of PDMS. Modified with permission from ref 105 under a Creative Commons Attribution License.

plasma-treated micropost arrays, which were coated with vitronectin. These cells were mechanosensitive and increased their cytoskeleton contractility with matrix stiffness, and stiff substrates were supportive of the maintenance of hESC pluripotency.<sup>105</sup> Matrix mechanics-mediated cytoskeleton contractility seems to be functionally correlated with E-cadherin expression in cell–cell contacts and involved in hESC cell fate decisions. The microenvironment of hESC culture on micropost arrays should be different than that of conventional 2-D culture.<sup>105</sup> This difference may lead to different optimal elasticities (stiffness) for the maintenance of hESC pluripotency, where stiff surfaces are preferable in micropost array culture and soft surfaces are preferable in conventional 2-D culture.

The *in vivo* microenvironment of hMSCs regulates their self-renewal and differentiation. Human MSCs cultured *ex vivo* gradually lose their pluripotency after 10–20 passages, as characterized by a lack of proliferation and differentiation. Winer et al. cultured hMSCs on 250-Pa cross-linked PAAm hydrogels coated with the ECM proteins fibronectin and collagen I. These hydrogels mimic the elasticity of bone marrow (220 Pa of storage modulus for bovine bone marrow) and fat tissues (Figure 2).<sup>87</sup> Human MSCs cultured on a soft substrate halted cell cycle progression, despite the presence of serum; these nonproliferative hMSCs re-proliferated when replated on a stiff substrate. Nonproliferative hMSCs on 250-Pa PAAm hydrogels also exhibited the capability to differentiate into adipocytes when cultured in adipogenic induction medium and differentiated into osteoblasts when incubated on a stiff substrate in osteoblast induction medium. These results demonstrate that hMSCs on soft (250-Pa) PAAm hydrogels

are quiescent but competent to resume proliferation or initiate terminal differentiation when provided with appropriate cues. These observations suggest that the biomaterial physical cue of ECM elasticity is a factor enabling the bone marrow niche to maintain a reservoir of hMSCs for long periods.<sup>87</sup>

### 2.3. Mechanism of Regulation of Stem Cell Differentiation Fate by ECM and Substrate Elasticity in 2-D Culture

The mechanism by which the elasticity of ECM on culture substrates induces lineage specification of stem cell differentiation is currently difficult to explain. Figure 7 illustrates several mechanosensing models proposed by several researchers for detecting substrate elasticity and the direction of different MSC lineages.<sup>60,72,74</sup> The elasticity of the ECM on the substrate generates mechanical stimuli on the plated stem cells, thereby inducing changes in focal adhesion (FA) protein activity and remodeling.<sup>72–75</sup> The growth and elongation of focal adhesions vary depending on culture substrate stiffness, suggesting that ECM elasticity regulates focal adhesion assembly (Figure 7). Integrins are known as the most important mechanical sensors positioned at the starting point of the sensing pathway.<sup>72</sup> Du et al. reported that  $\beta 1$  integrin activation in MSCs was induced by soft culture substrate to a significantly greater degree than by stiff culture substrate.<sup>72</sup> However, the level of cell-surface integrins in MSCs on soft culture substrate was significantly lower than that on stiff culture substrate in 2-D culture (Figure 7). Soft substrate markedly enhanced the internalization of integrin; this internalization was mediated mainly through caveolae/raft-dependent endocytosis.<sup>72</sup> Enhanced integrin internalization in MSCs on soft culture substrate guides neural differentiation of MSCs by inhibiting the bone morphogenetic protein (BMP)–Smad pathway. The inhibition of integrin internalization by the caveolae/raft inhibitor methyl- $\beta$ -cyclodextrin was found to block neural lineage differentiation of MSCs on soft substrate in 2-D culture. Soft substrate suppressed the BMP–Smad pathway partially via integrin-regulated BMP receptor endocytosis.<sup>72</sup>

Atomic force microscopy data suggested that integrin–receptor complexes are more easily ruptured on soft culture substrates than on stiff culture substrates. This phenomenon may contribute to the enhancement of integrin internalization on soft culture substrates. It has been suggested that ECM elasticity affects the integrin activity of MSCs and trafficking mechanisms modulating integrin–receptor internalization, thereby contributing to the specific lineage differentiation of

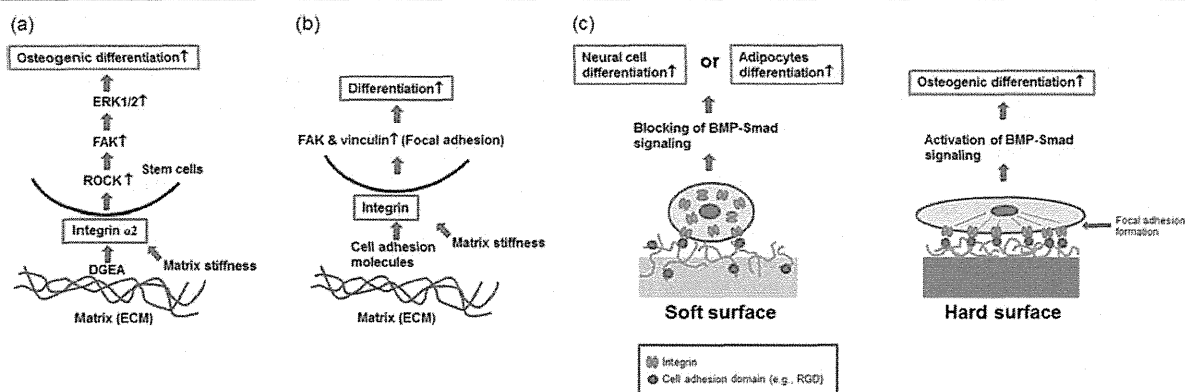


**Figure 7.** The mechanism of the effect of culture substrate stiffness on stem cell differentiation via the growth and elongation of focal adhesions, as suggested by Shih et al. (a),<sup>74</sup> Yim et al. (b),<sup>60</sup> and Du et al. (c).<sup>72</sup>

stem cells cultured on ECM with specific elasticities in 2-D culture.<sup>72</sup>

#### 2.4. Elasticity of Substrate Directs Stem Cell Differentiation Fate in 3-D Culture

Elasticity of scaffolds is another important factor for specific lineage differentiation of stem cells in three-dimensional (3-D) culture.<sup>63</sup> Several researchers have reported that the stiffness of cell culture scaffolds (matrix) affects specific stem cell differentiation lineages in 3-D culture.<sup>59,63–65,70,77,98,102</sup>

Murphy et al. prepared cross-linked collagen–glycosaminoglycan scaffolds as analogues of natural ECM. Two different glycosaminoglycans, chondroitin sulfate (CS) and hyaluronic acid (HyA), were used.<sup>63</sup> Cross-linking with dehydrothermal (DHT) treatment and 1-ethyl-3-(3-dimethyl aminopropyl) carbodiimide (EDAC) produced three collagen–glycosaminoglycan scaffolds with stiffness values of 0.5, 1, and 1.5 kPa. In their study, the effect of scaffold stiffness and glycosaminoglycan composition on rat MSC differentiation was investigated in expansion medium in the absence of induction (differentiation) supplements.<sup>63</sup> The scaffolds prepared with HyA and with the lowest stiffness (0.5 kPa) facilitated a significant upregulation in Sox9 expression, indicating that MSCs were directed toward a chondrogenic lineage. In contrast, Runx2 expression was highest in the stiffest (1.5 kPa) scaffolds prepared with CS, indicating that MSCs were directed toward an osteogenic lineage in stiffer scaffolds.<sup>63</sup> This study demonstrated that scaffold stiffness can direct MSC fate in 3-D culture even in the absence of differentiation supplements; this capability is further enhanced by the selection of optimal scaffold components for specific differentiation lineages.

An injectable and biodegradable hydrogel composed of hyaluronic acid–tyramine (HyA-Tyr) conjugates was prepared by Toh et al.<sup>64</sup> HyA-Tyr was cross-linked *in vivo* by the addition of small amounts of peroxidase and hydrogen peroxide (H<sub>2</sub>O<sub>2</sub>) with independent tuning of the gelation rate and the degree of cross-linking, both of which affected hydrogel elasticity.<sup>64</sup> HyA-Tyr hydrogels of varying elasticities (5.4, 9.5, and 11.8 kPa) were explored as biomimetic matrices for caprine MSCs in cartilage tissue engineering where the compressive modulus, equilibrium swelling, and degradation rate were controlled by varying the concentration of H<sub>2</sub>O<sub>2</sub> as the oxidant in the oxidative coupling reaction (Figure 8).<sup>64,120</sup> Cellular condensation, which was determined by measuring the increase in the effective number density of rounded cells in the lacunae, was found to enhance in softer hydrogel matrices with lower cross-linking that displayed enhanced scaffold contracture. Conversely, cells expressed a more elongated morphology with a reduced degree of cellular condensation in more highly cross-linked matrices.<sup>64</sup> The degree of hydrogel cross-linking also modulated matrix biosynthesis and cartilage tissue histogenesis. Matrices with less cross-linking enhanced chondrogenesis, demonstrating increases in the percentage of cells with chondrocyte morphology and increases in the biosynthetic rates of glycosaminoglycan and collagen type II where hyaline cartilage tissue formation was observed.<sup>64</sup> It may be that the tunable three-dimensional microenvironment of the HA-Tyr hydrogels modulates cellular condensation during chondrogenesis and has an impact on cell spatial organization and matrix biosynthesis.

Pek et al. created thixotropic poly(ethylene glycol)–silica (PEG–silica) nanocomposite hydrogels with and without the cell adhesive RGD (Arg–Gly–Asp) oligopeptide for 3-D cell

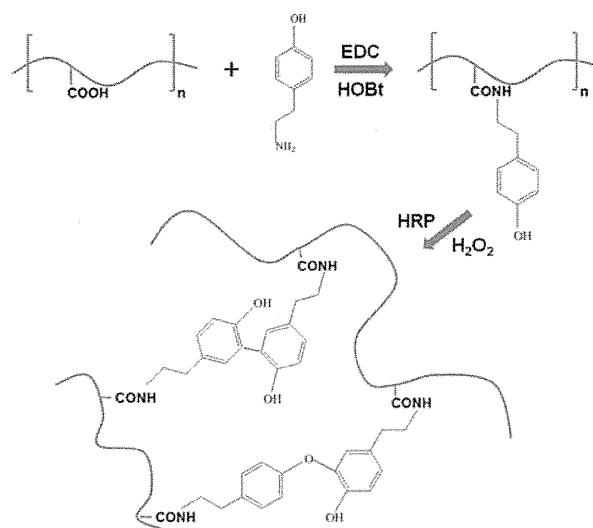


**Figure 8.** Preparation of hyaluronic acid–tyramine (HyA-Tyr) hydrogels in which their elasticity was controlled by varying the H<sub>2</sub>O<sub>2</sub> concentration as the oxidant in the oxidative coupling reaction with HRP as an enzyme. Modified with permission from ref 120. Copyright 2005 Royal Society of Chemistry.

culture.<sup>59</sup> The thixotropic PEG–silica hydrogel can be liquefied simply by applying a shear stress. This allows stem cells in the thixotropic hydrogels to be easily introduced into defect parts in human body before the matrix material reverts to a gel state. The matrix stiffness of the hydrogel can be tuned by controlling the amount of fumed silica in the hydrogel. Hydrogels were created with 7, 25, 40, 75, and 100 Pa of liquefaction stress, where the liquefaction stress is defined as the minimum shear stress at which the hydrogels become liquid under the conditions of storage modulus ( $G'$ ) = loss modulus ( $G''$ ) and  $\tan^{-1}(G''/G') = 45^\circ$ .<sup>59</sup> When hMSCs were cultured in PEG–silica nanocomposite hydrogel in expansion medium for 1 week, the highest expression level of neural transcript factor ENO2 was observed in hMSCs cultured in hydrogels with the lowest liquefaction stress (7 Pa).<sup>59</sup> Furthermore, the highest expression levels of myogenic (MYOG) and osteogenic (Runx2 and osteocalcin) transcription factors were observed in hMSCs cultured in intermediate (25 Pa) and high liquefaction stress (75 and 100 Pa) hydrogels, respectively. All of the aforementioned transcription factors were expressed more highly in hMSCs cultured in the PEG–silica nanocomposite hydrogel than in hMSCs cultured on conventional 2-D tissue culture polystyrene plates (TCPS). This result indicates that hMSCs cultured in 3-D are in a more differentiated state compared with cells cultured in 2-D. Immobilization of the cell-adhesion peptide RGD promoted both proliferation and differentiation of hMSCs on the stiffer hydrogels (liquefaction stress >75 Pa).<sup>59</sup> It was concluded that matrix stiffness (elasticity) regulates hMSC differentiation fate when cultured in 3-D PEG–silica nanocomposite hydrogel in expansion medium. In their study, it was demonstrated that mechanical signals alone can control lineage specification of hMSCs in 3-D culture. It was proposed that the mechanism by which RGD promotes osteogenesis is via its role as a ligand to the integrin mechanoreceptor, allowing stem cells to detect high matrix stiffness for bone differentiation.